

NWP SAF

Satellite Application Facility for Numerical Weather Prediction Associate Scientist Mission Report

Document NWPSAF-MO-VS-028

Version 2.2

20 December 2005

Implementation Plan for a NRT global ASCAT soil moisture product for NWP

Part 4: Discrete Global Grid Systems

R A Kidd

Institute of Photogrammetry and Remote Sensing, Vienna University
of Technology, Austria.



ASCAT Soil Moisture Report Series No. 4

Discrete Global Grid Systems

VIENNA
UNIVERSITY OF
TECHNOLOGY

INSTITUTE OF
PHOTOGRAMMETRY
AND REMOTE SENSING



2005 December 20

How to reference this report:

Kidd, R. (2005). *NWP Discrete Global Grid Systems*. ASCAT Soil Moisture Report Series, No. 4, Institute of Photogrammetry and Remote Sensing, Vienna University of Technology, Austria.

Contact Information:

Institute of Photogrammetry and Remote Sensing (I.P.F.)
Remote Sensing Group (Prof. Wagner)
Vienna University of Technology
Gusshausstrasse 27-29/E122
1040 Vienna, Austria

mbox@ipf.tuwien.ac.at
www.ipf.tuwien.ac.at

Status:	Issue 2.2		
Authors:	IPF TU Wien (RAK)		
Circulation:	IPF, NWP and others		
Amendments:			
<i>Issue</i>	<i>Date</i>	<i>Details</i>	<i>Editor</i>
Issue 1.1	2005 Feb	Draft Version.	RAK
Issue 1.2	2005 July	Complete restructure of document	RAK
Issue 2.0	2005 Dec	Draft for internal IPF comments	RAK
Issue 2.2	2005 Dec 20	Draft for external comments	RAK

If further corrections are required please contact Richard Kidd (rk@ipf.tuwien.ac.at).

Abstract

This report presents a proposal for a new discrete global grid (DGG) that is recommended for implementation within IPF's software for processing scatterometer data and generating soil moisture products. The new grid is to improve the current adapted sinusoidal grid used within WARP4.0.

An overview of the three main methods for implementing DGG's; partitioning, tiling and subdivision, is presented and their benefits and limitations are discussed. Four candidate DGG's are selected which represent the current state of the art both within IPF's operational processing environments and within the larger scientific community. This includes the proposed SMOS grid.

The candidate grids are assessed based upon a detailed set of requirements and considerations for operational processing of scatterometer data. A simple compliancy matrix determines that the best potential DGG is the QSCAT grid which was implemented by IPF for the extraction and processing of NASA's QuikSCAT scatterometer data.

The report concludes with the presentation of the proposed WARP5 grid, which is an adapted geodetic grid based upon the GEM6 ellipsoid, and includes a detailed description on the grid generation and an assessment of intergrid distances.

The present study was funded by the NWP SAF (<http://www.metoffice.com/research/interproj/nwpsaf>).

List of Acronyms and Abbreviations

AARI	Arctic and Antarctic Research Institute
ASCAT	Advanced Scatterometer
ASPS	Advanced Scatterometer Processing System
AVHRR	Advanced Very High Resolution Radiometer (for visible and infrared imagery, flown in polar orbit)
DEM	Digital Elevation Model
DGG	Discrete Global Grid
DGGS	Discrete Global Grid System
DTED	Digital Terrain Elevation Data
EASE	Equal-Area Scalable Earth Grid
ERBE	Earth Radiation Budget Experiment
ESCAT	ERS Scatterometer
ETOPO2	Earth Topography - 2 Minute
GEM6	Goddard Earth Model 6
GLOBE	Global Land One-km Base Elevation Project
GRS 80	Geodetic Reference System 1980
IDL	Interactive Data Language
IPF	Institut für Photogrammetrie und Fernerkundung - Institute of Photogrammetry and Remote Sensing
ISEA	Icosahedron Snyder Equal Area
ISEA3H	Icosahedron Snyder Equal Area Aperture 3 Hexagonal DGGS
ISEA4H	Icosahedron Snyder Equal Area Aperture 4 Hexagonal DGGS
METOP	Meteorological Operational satellite
MODIS	Moderate Resolution Imaging Spectroradiometer
NASA	National Aeronautics and Space Administration (USA)
NIMA	National Imagery and Mapping Agency (USA)
NRT	Near-Real Time
NSIDC	National snow and ice data centre
NWP	Numerical Weather Prediction
QSCAT	QuikSCAT
QTM	Quaternary Triangular Mesh
RADLAB	University of Michigan Radiation Laboratory
SAF	Satellite Application Facility
SMMR	Scanning Multichannel Microwave Radiometer
SMOS	Soil Moisture and Ocean Salinity
SSM/I	Special sensor Microwave/Imager
TOVS	TIROS Operational Vertical Sounder
UWI	Wind Scatterometer Fast Delivery Product
WARP	WATER Retrieval Package
WGS84	World Geodetic System 84
WMO	World Meteorological Organization (UN)

Related Documents

For more information relating to IPF's work concerning the derivation of Soil Moisture products from ASCAT data the reader is directed to the reports detailed in Table 1-1.

Report Series No.	Report Title
1	Kidd, R. (2005). <i>NWP User Community Requirements Summary.</i>
2	Kidd, R. (2005). <i>METOP ASCAT Data Streams and Data Formats.</i>
3	Bartalis, Z. (2005). <i>Azimuthal Anisotropy of Scatterometer Measurements over Land.</i>
5	Wagner, W. (2005). <i>Implementation Plan for a Soil Moisture Product for NWP</i>
6	Bartalis, Z. (2005). <i>Selection of Resampling Procedure.</i>
7	Scipal, K. et al. (2005). <i>Definition of Quality Flags.</i>
8	Hasenauer, S., et al. (2005). <i>WARP-NRT 1.0 Reference Manual.</i>

Table 1-1
ASCAT Soil Moisture Report Series.

Contents

Abstract	i
List of Acronyms and Abbreviations	ii
Related Documents	iii
Contents	iv
1 Introduction and Statement of Requirements	1
1.1 Statement of Requirements	1
2 Discrete Global Grids and Systems	3
2.1 What is a Discrete Global Grid?	3
2.1.1 Grid Characteristics	3
2.2 Discrete Global Grid Systems	4
3 Discrete Global Grid Overview	6
3.1 Partitioning	6
3.2 Tiling	8
3.3 Subdivision	11
3.4 Summary	14
4 Candidate Grids	16
4.1 The WARP4 Grid	16
4.1.1 Grid Summary	17
4.2 The QSCAT Grid	18
4.2.1 Grid Summary	19
4.3 The EASE Grid	20
4.3.1 Grid Summary	22
4.4 The SMOS Grid	23
4.4.1 Grid Summary	24
5 Considerations for Grid Generation and Use	25
5.1 Ellipsoid or Sphere	25
5.2 Point Location and Grid Indexing	26
5.3 Grid Generation	27
5.4 Global Coverage	29
6 Comparison of Candidate Grids	30
6.1 Consideration of Grid Requirements	30
6.1.1 Grid Requirements	30
6.1.2 Redundant Grid Requirements	30
6.2 Assessment of Candidate Grids	31
7 Proposed Grid	33
7.1 The WARP5 grid	33
7.1.1 Grid Summary	34
7.2 Variation of Intergrid Distance	34

Bibliography	37
Annex A: Intergrid Distance.....	I

1 Introduction and Statement of Requirements

The Institute of Photogrammetry and Remote Sensing (I.P.F.) of the Vienna University of Technology (TU Wien) has been developing algorithms and software for producing soil moisture data from ERS-1/2 scatterometer data since 1994. The software for processing the scatterometer data is called WARP (soil *W*ater *R*etrieval *P*ackage) and is written entirely in the software language IDL (Interactive Data Language).

The most distinct feature of WARP is that all processing is done in the time domain. Since scatterometer data arrive in an image format, with satellite geometry, the data need to be reorganised from an image to a time series format in the first processing step. In order to organise backscatter time series, measurements must be spatially aggregated into sets of regions (so-called grid areas) that partition the surface of the Earth in an approximately regular manner. Such regions form a Discrete Global Grid (DGG). Each defined grid area is associated with time series of backscatter measurements and holds its own entry in the backscatter metadata database.

As part of the continuing development of the WARP package this document focus upon the assessment and recommendations for the improvement of the current DGG, described in section 4.1, that is used in WARP 4.0.

1.1 Statement of Requirements

The design or selection of an appropriate Discrete Global Grid depends upon the consideration of a number of requirements. In the following section we outline the requirements for a DGG for I.P.F.'s soil moisture product and present specific implications of these requirements.

Coverage: The grid should be provided by a *single solution* and offer a global coverage.

Equal Area: The full information content of the input data should be maintained. This implies uniformly spaced isotropic *equal area grid*

at (at least) *twice instrument resolution* from which the data is received.

Coordinate system: Coordinate transformation and data location errors should be minimised. The grid should be presented in the *same coordinate system as the input satellite data*.

Grid Spacing: Interpolation errors due to regridding should be minimised. This requires *uniform grid spacing*.

Data Access: The requirement for near real time product generation means that the grid design must allow effective handling and gridding of large scatterometer input data sets, transfer of data from the orbital data coordinate system to grid system and from grid to orbit coordinate system. This implies *efficient method for grid indexing or point location* allowing straightforward and timely retrieval of grid data.

Resolution: The capability to sufficiently *increase or decrease resolution of the grid*, to resolve scales of interest should be considered. This raises the question if a congruent grid should be employed.

Resampling: It should be possible to *resample the grid in a meaningful manner to any other grid*. This will afford maximal possibly for product validation or comparison, either within house, or within the general scientific community.

Knowledge Transfer: *Heritage*, in terms of knowledge and technology, from I.P.F.'s in-depth experience developing and working with adapted sinusoidal grids *should be fully exploited*.

2 Discrete Global Grids and Systems

The ability to specify geographic location is fundamental to many areas of science, government, and commerce. Traditional approaches to represent geospatial location on computers, such as planar map projection coordinates and the latitude/longitude system have limitations when used to reference the high resolution global data sets which are now becoming increasingly common. Discrete Global Grids (DGG) are a new class of geospatial data structures based on regular, and often hierarchical, partitions of the Earth's surface. DGGs have the potential to enable faster, more efficient, and more accurate solutions in a variety of disciplines.

2.1 What is a Discrete Global Grid?

A Discrete Global Grid consists of a set of regions that form a partition of the Earth's surface, where each region has a single point contained in the region associated with it. Each region/point combination is a cell (Sahr, K., White, D., and Kimerling, A. J., 2003). Cell regions may vary in shape from irregular shapes, such as the division of the Earth's surface into land masses and bodies of water, to regular regions with evenly distributed points. In this document we will focus only on regular DGG's as these are unbiased with respect to spatial patterns created by natural or anthropogenic processes and allow for the development of simple and efficient algorithms.

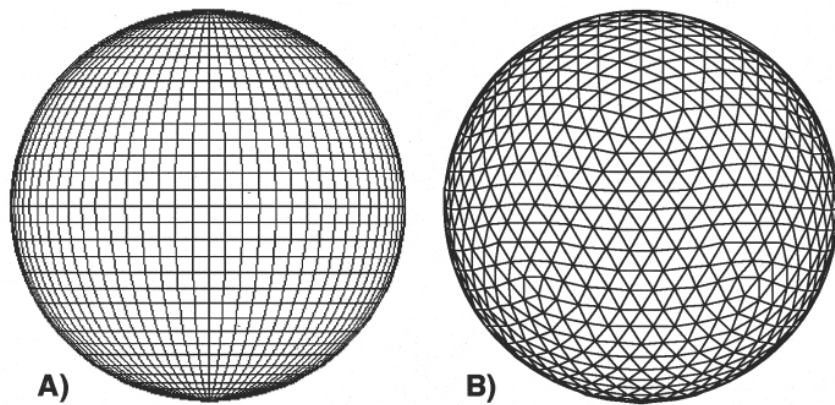
To provide a common understanding for all readers the following sub sections briefly introduce some key terms that are commonly used when defining or describing DGG's.

2.1.1 Grid Characteristics

Orientation is the property of cells maintaining coherence of direction along the spatial partitioning. A square lattice would be uniformly oriented whereas a triangular one would not.

Figure 2-1.

Two grid systems used with paleoclimatic data: A) 5° by 5° orthogonal grid exhibiting uniform orientation, and B) an icosahedral spherical grid subdivided by triangles. (adapted from Moore, T., L., 1998)



Adjacency is a measure of the relation between a cell and its neighbours. A grid possessing uniform adjacency means that a cell with n edges also has n neighbours. A non-uniform grid means that each cell has some neighbours with which only shares vertices.

Figure 2-2.

Regular polygon cells used within DGG (adapted from Randall, D.A., Ringler, T.D., Heikes, R.P.; Jones, P and J. Baumgardner, 2002,)



Hexagonal cells can be used to generate a uniform highly symmetric grid. Each cell shares both vertices and cell walls with its 6 neighbours. Square cells, with 8 neighbours and 4 wall neighbours and triangular cells with 12 neighbours and 3 wall neighbours have lower degrees of symmetry.

2.2 Discrete Global Grid Systems

A Discrete Global Grid System (DGGS) is a series of discrete global grids which usually consist of increasingly finer resolution grids. If these grids are defined consistently using regular planar polygons then the **aperture** of the DGGS can be defined as the ratio of the areas of planar polygon cell at resolution k and resolution $k+1$, or simply stated the aperture is the number of shapes chosen to sub divide two consecutive resolutions. Three levels of an aperture 4 triangle is presented in Figure 2-3.

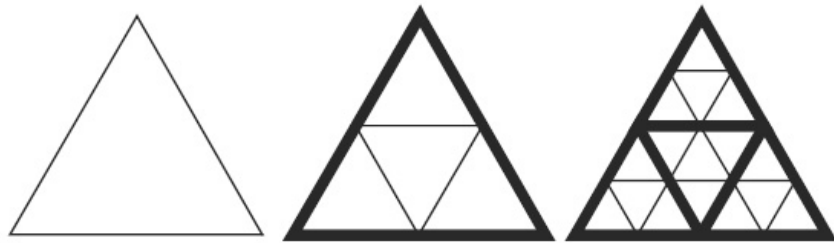


Figure 2-3.

Three levels of an aperture 4 triangle subdivision. (adapted from Sahr, K., and White, D., 1998)

In order to create efficient data structures within DGGS resolutions a regular hierarchical relationship is important. The two most common types of relationships within DGGS are that of alignment or congruency.

Alignment is the property of a cell point in resolution n also being a cell point in resolution $n+1$.

Congruency is the capability of decomposing a cell of resolution n into smaller cells of resolution $n-1$, or their aggregation into larger cells of resolution $n+1$. A triangular grid would be congruent whereas a hexagonal grid would not.

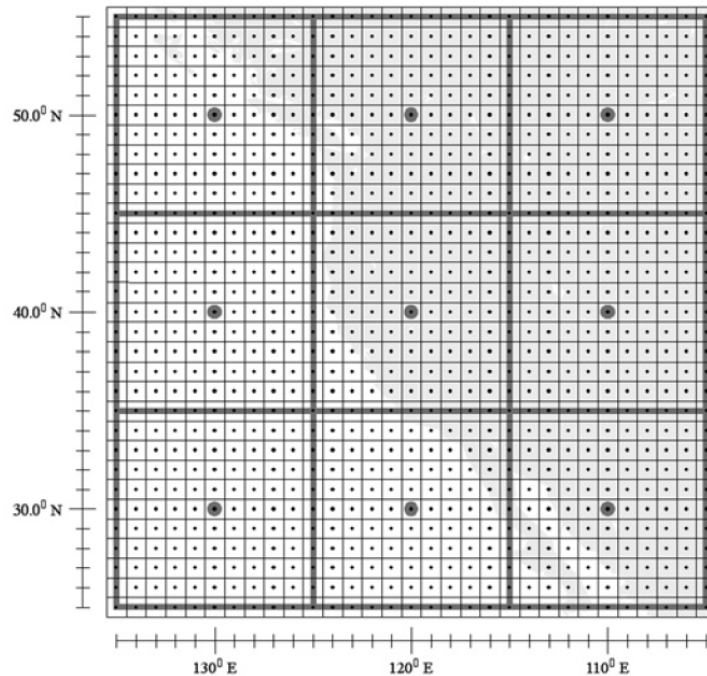


Figure 2-4.

Section of a two resolution DGGS (adapted from Sahr, K., White, D., and Kimerling, A. J., 2003)

Figure 2-4 shows a two resolution (10° and 1°) DGGS with a geographic coordinate system. This is an example of a DGGS with an incongruent, aligned hierarchy.

3 Discrete Global Grid Overview

There are many different types of discrete global grids each with different properties and therefore different “best” uses, but as discussed by Suess, M., Matos, P., Gutierrez, A., Zundo, M., and Martin-Neira, M., 2004 global grids are generally obtained by one of three main techniques. The Globe may be either; partitioned into geographic lat-long coordinate systems; or once in a specified projection the Globe may be tiled with a square lattice; or finally the Globe may be inscribed by a platonic solid whose faces are then subdivided into regular shapes, such as triangles, diamonds or hexagons.

In the following section each of these methods is presented along with common examples of usage and the benefits and limitations associated with each method are discussed.

3.1 Partitioning

The most commonly used regular DGG’s, are those based on geographic coordinate system i.e. partitioning of the globe into latitude-longitude coordinate system (Sahr, K., White, D., and Kimerling, A. J., 2003).

DGG’s based on geographic coordinate system have numerous practical advantages. Historically the geographic coordinate system is a well known and well used coordinate system and is the basis for a varied number of data sets and processing software. The two dimensional map of the geographic projection is termed the Plate Carree projection as shown in Figure 3–1. Grids based on square partitions are familiar and map effectively to common data structures and display devices. Raster data sets, for example NASA Earth Radiation Budget Experiment (ERBE) grids, are often based upon cell regions with edges defined by arcs of equal angle increments of latitude and longitude (for example, $2.5^\circ \times 2.5^\circ$, $5^\circ \times 5^\circ$ or $10^\circ \times 10^\circ$), or the Global Land One-km Base Elevation (GLOBE) Project; a 30-arc-second (1-km) gridded, quality-controlled global Digital Elevation Model (DEM) referenced to the World Geodetic System 84 (WGS84). Data values may also be associated with points spaced at equal angle intervals of latitude and longitude, for example the $2' \times 2'$ ETOPO2 gridded global relief data set.

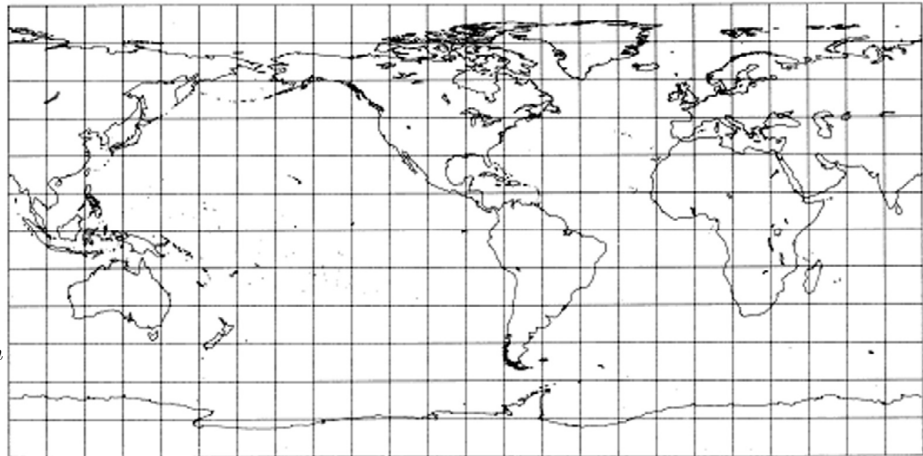


Figure 3-1.

Geographic, or Plate Carree projection with 15° graticule. Central meridian 90° W. (adapted from <http://www.3dsoftware.com/>, image from Snyder, J.,P., 1997)

No map projection maintains correct scale throughout. It is important to accurately visualize how different parts of a map are distorted. This can be done with the Tissot Indicatrix, which is a small circle that when plotted on a map will appear as an ellipse (elongated circle) if that point on the map is distorted. The circle becomes elongated in the direction of the angular distortion, and becomes larger or smaller if the size of the area is distorted at the center of the circle. A series of these circles can be plotted on a map to visualize distortion throughout the map.

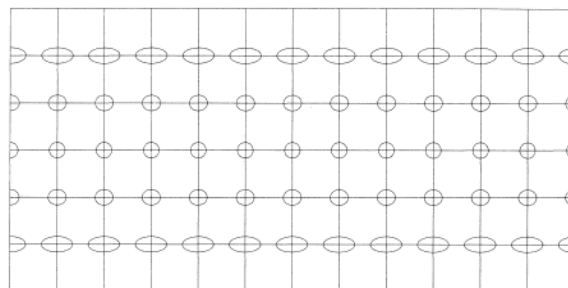


Figure 3-2.

A Tissot Indicatrix plot for the Geographic, or Plate Carree projection (adapted from <http://www.3dsoftware.com/>)

The Tissot Indicatrix plot Figure 3-2 for the geographic projection clearly displays the inherent distortions in a grid system based upon the partitioning of the Globe into the geographic coordinate system. The indicatrices (distortion circles) along the Equator are perfect circles. That is the only parallel (latitude) of true scale on this projection. In parallels other than the Equator, the indicatrices widen, showing that land areas are stretched horizontally on the map at those latitudes. As shown in Figure 3-2 DGG's created by the latitude-longitude grid do not have equal area cell regions with cells becoming increasingly distorted in area, shape, and interpoint spacing as you move away from the equator.

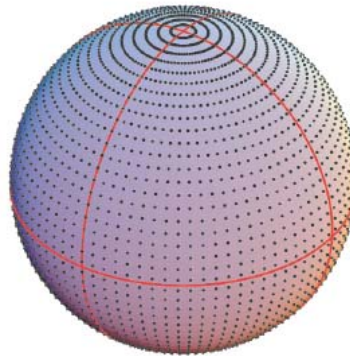
Partitioning results in a square grid cell. The square cells produced by this latitude longitude grid do not exhibit uniform adjacency A square grid cell has four neighbours with which it shares an edge, and

whose centers are equidistant from its' center. But each cell also has four neighbours with which it only shares a vertex and whose centers are a different distance from its center than the distance to the centre of the edge neighbours (Sahr, K., and White, D., 1998).

Finally, it can be seen in Figure 3–3. that polar singularities exist at the north and south poles in which the poles map to lines on the latitude and longitude plane.

Figure 3-3.

An example of a latitude-longitude grid with black dots representing grid cells centres equally spaced in longitude and latitude. (adapted from Randall, D.A., Ringler, T.D., Heikes, R.P.; Jones, P and J. Baumgardner, 2002,



Numerous adapted DGG's based upon the geographic latitude longitude grid have been implemented to address some of the inherent limitations. One such adaptation was to decrease the number of cells with increasing latitude to achieve more consistent cell size. The Digital Terrain Elevation Data DTED (MIL-PRF-89020B, 2000) from NIMA, is based on an evenly spaced quadrilateral grid of points, but with the globe split into latitudinal zones with varying horizontal distances between grid lines; a similar approach was also implemented to derive the FFI grid (Bjørke, J. T., Grytten, J. K., Hæger, M., and Nilsen, S., 2003

Despite the known problems associated with these type of DGG's the adapted partitioning approach is found to be an appropriate solution for some data sets, such as noted by the developers of the FFI approach. They state that adapted partitioning is an appropriate solution since the grid covers the whole globe with cells of approximately the same size, the relationship between the grid and the latitude longitude system is simple and the grid system supports a matrix representation.

3.2 Tiling

With the application of more complex projection systems the partitioning technique evolved into a technique known as tiling. The Globe, once in a specified projection, is tiled with a square lattice which forms a DGG.

Before discussing common tiling approaches it is useful to reflect upon some common properties of projection systems. A map projection

will either optimise equal area, true shape, true distance or will provide a compromise between them. Equal area, or equivalence, means that areas on one part of the map are in scale with areas in any other zones. Preservation of equivalence involves inexact transformation of angles around points and thus, is mutually exclusive with true shape, or conformality, except along one or two selected lines.

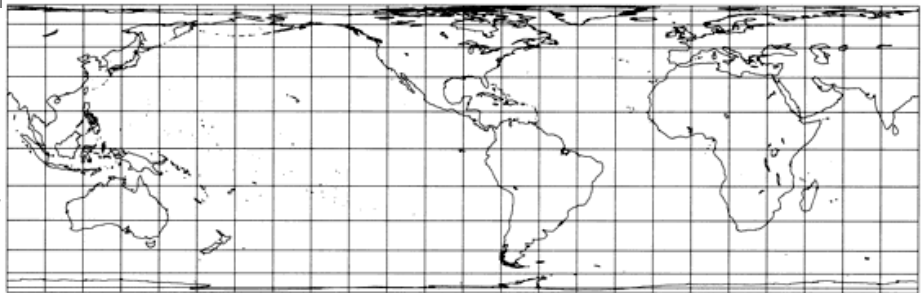
Conformality is the characteristic of true shape or, in other words, how well does the projection preserves the shape of a geographical area? This is achieved through the exact transformation of angles around points, with the necessary condition that the intersection be perpendicular to the grid lines; as on the globe. A projection with the true shape feature is said to be conformal. The characteristic of true distance or equidistance means that the scale of distance is constant over the entire map. This property can be fulfilled on any given map from one, or at most two, points in any direction or along certain lines. Usually, reference lines such as the equator or a meridian are chosen to have equidistance.

For global applications the most important characteristic of a map projection is that of equal area or equivalence. Area preserving projections, such as cylindrical equal area projections are preferred.

The Cylindrical Equal-Area Projection, Figure 3-4., was proposed by Johann Heinrich Lambert in 1772. It has seldom been used, except as a textbook example of the most easily constructed equal-area projection, but several modifications have been published and are widely used.

Figure 3-4.

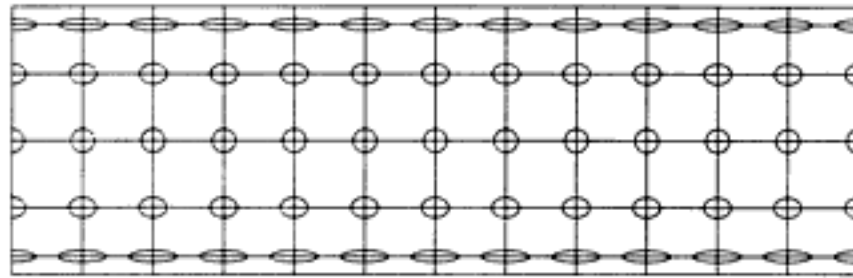
Lambert Cylindrical Equal-Area projection with 15° graticule. Standard parallel 0° . Central meridian 90° W



The modifications consist of compressing the projection from east to west and expanding it in the same ratio from north to south, thereby moving the parallel of no distortion (standard parallel) from the Equator to other latitudes.

Figure 3-5

Tissot Indicatrix for Lambert Cylindrical Equal-Area projection, 30° graticule Standard parallel 0°

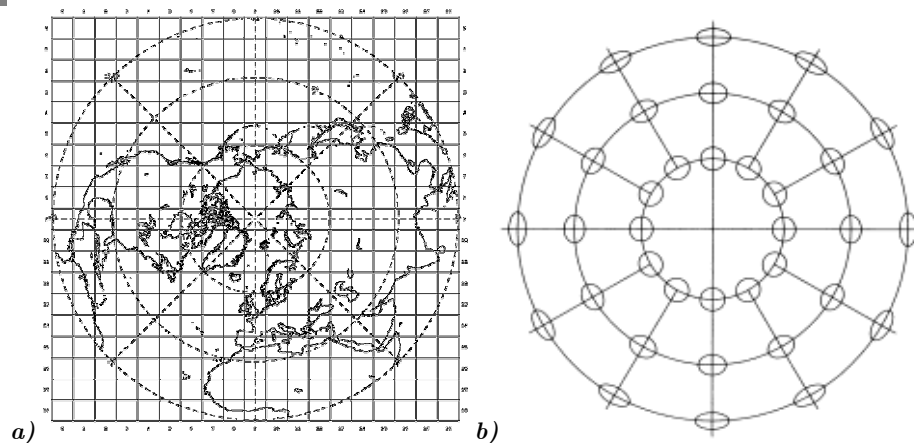


As an example of one of the more commonly known tiled DGG's, the Equal-Area Scalable Earth Grid (EASE-Grid) grid uses a cylindrical equal area projection with two standard parallels at $\pm 30^\circ$ Lat.

As mentioned by (Bjørke, J. T., Grytten, J. K., Hæger, M., and Nilssen, S., 2003) when considering projections with a global extent projection errors may be considerable, and so it is also common to find tiled grids that focus on specific regions of the globe. In these cases the map projection selected seeks to minimise projection distortions for the area of interest. The Polar grid, selected for the MODIS data set, is shown in Figure 3-6, The polar regions are projected into a Lambert Azimuthal Equal area projection before being tiled into a DGG.

Figure 3-6.

a) Polar Lambert Azimuthal Equal-Area projection, with 45° graticule. Central meridian 0°E b) Tissot Indicatrix for projection.



Global projections have inherent limitations, as shown in Figure 3-5 with the wider indicatrices above and below 60° of latitude signifying areal distortion. To overcome distortions within a single projection for a global DGG one approach is to use a merged projection and then apply tiling to generate a DGG. An example concerns the Global Land 1-KM AVHRR Project which employs the Interrupted Goode Homolosine projection.

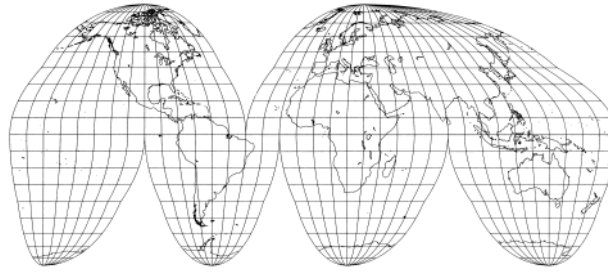


Figure 3-7.

Goode Homolosine projection with 10° graticule

The Interrupted Goode Homolosine projection, developed by J.P. Goode in 1923, is an equal-area pseudocylindrical composite map projection which is interrupted to reduce distortion in the major land masses. This projection merges the Mollweide projection for higher latitudes (also called the Homolographic projection) and the Sinusoidal projection for lower latitudes. The two projections join at 40° 44' 11.8" North and South; this is where the linear scale of the two projections match. All the major continents, with the exception of Antarctica, are intact. An ellipsoid distortion plot, similar to the Tissot Indicatrix is shown in Figure 3-8.

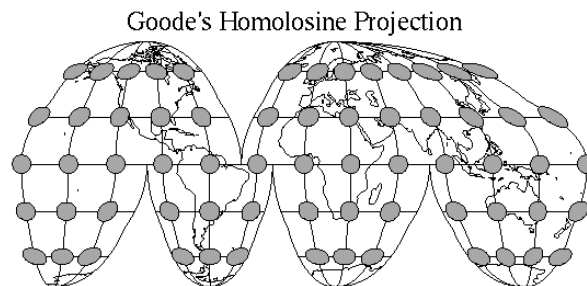


Figure 3-8.

A Tissot Indicatrix for Goode Homolosine projection (adapted from Steinwand, D.R.,)

In both the uninterrupted Sinusoidal projection and the uninterrupted Mollweide projection, the areas of maximum distortion are symmetrically positioned in the outer portions of the projections' four quadrants. In the Interrupted Goode Homolosine, these regions of higher distortion are avoided by using the central portions of these projections. In addition, combining the Sinusoidal projection, which presents shapes more accurately in the equatorial regions, with the Mollweide projection, which presents shapes more accurately in the higher latitudes, further minimizes distortion. By using the Interrupted Goode Homolosine projection the Global Land 1-KM AVHRR Project has DGG tiled with 17347 rows and 40031 columns at 1km resolution

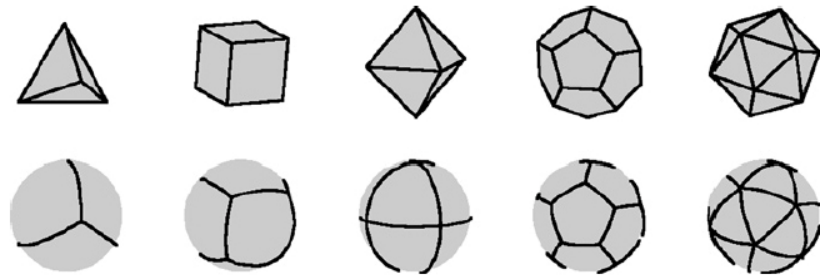
3.3 Subdivision

The final method considered here to generate a DGG is to represent the Globe as a sphere and then partition the sphere into cells each con-

sisting of the same regular spherical polygon with the same number of polygons meeting at each vertex. Each face of the polygon is then tiled with uniform cells, the resolution of the DGG is determined by the number of cells used to tile the faces. When the DGG has more than one resolution it is classed as a DGGS. As noted by Sahr, K., and White, D., 1998 , Sahr, K., White, D., and Kimerling, A. J., 2003 and many others, there are only five platonic solids which can be used for this, as shown in Figure 3–9.

Figure 3–9.

Planar and spherical versions of the five platonic solids; the tetrahedron, the hexahedron, octahedron, dodecahedron, and icosahedron. (adapted from Sahr, K., White, D., and Kimerling, A. J., 2003)

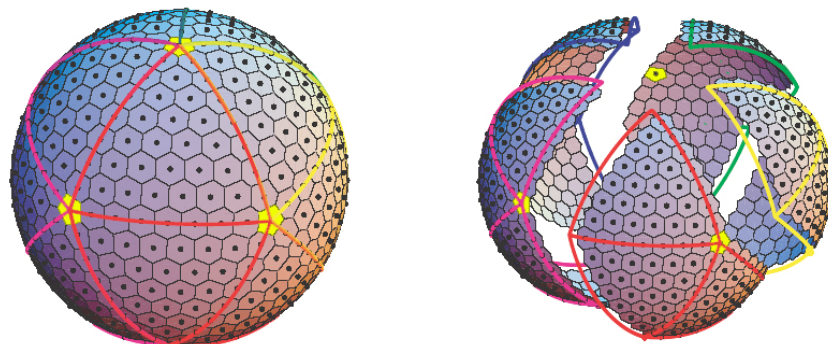


The most common approach, as determined from Table 3–1, tends to be based upon the selection of the icosahedron as a base platonic solid. The octahedron has also been widely used; for example the Quaternary Triangular Mesh (QTM) was developed with an octahedron as the base platonic solid.

In Randall, D.A., Ringler, T.D., Heikes, R.P.; Jones, P and J. Baumgardner, 2002, the icosahedron is selected and hexagonal cells are then used to tile each face. In the resulting grid it is noted that there numerous hexagonal cells and 12 pentagonal cells, which, as highlighted in Figure 3–10, are formed at the intersecting nodes of each face of the icosahedron.

Figure 3–10.

Spherical Geodesic Grid, based on an icosahedron tiled with Hexagons. Pentagons are noted at the intersection of each face. (adapted from Randall, D.A., Ringler, T.D., Heikes, R.P.; Jones, P and J. Baumgardner, 2002,)



Presenting pairs of faces in logical rectangular panels, Figure 3–11, offers a convenient way to organise data within a computer Randall, D.A., Ringler, T.D., Heikes, R.P.; Jones, P and J. Baumgardner, 2002, . As discussed in Sahr, K., White, D., and Kimerling, A. J., 2003, since many of these DGGS have adapted from work undertaken by the renowned American architect R. Buckminster Fuller in developing a geodesic dome, this class of DGGS is termed Geodesic DGGS.

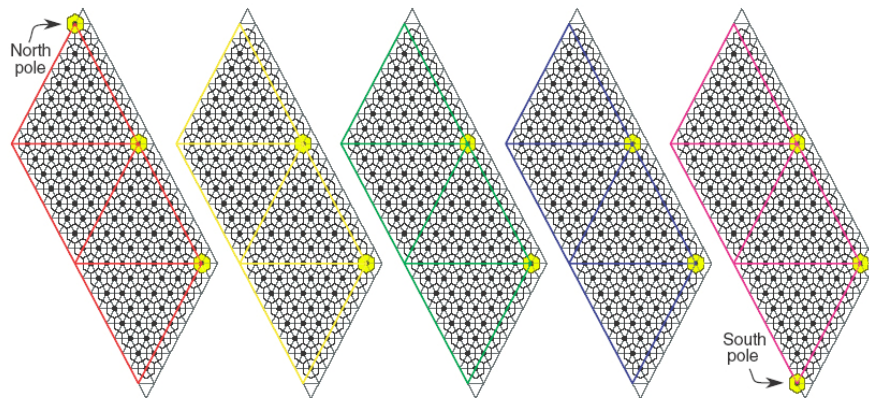


Figure 3-11.
Spherical Geodesic Grid, presented as logical rectangular panels (adapted from Randall, D.A., Ringler, T.D., Heikes, R.P.; Jones, P and J. Baumgardner, 2002,)

There have been numerous applications of Geodesic DGGS in various fields of applications, some of which are summarised in Table 3-1, but according to Sahr, K., White, D., and Kimerling, A. J., 2003 all are constructed based upon five design choices. It is noted that there is unlikely to be a single optimal DGGS for all applications.

The design choices that must be made to fully specify a Geodesic DGGS comprise:

- The base platonic solid
- The orientation of the base platonic solid relative to the Earth
- The hierarchical spatial partitioning method defined symmetrically on a face, or set of faces, of the base platonic solid
- The transformation between each face and the corresponding spherical surface.
- The definition of a point to identify each cell

Table 3-1

Summary of Geodesic DGGS design choices (adapted from Sahr, K., White, D., and Kimerling, A. J., 2003)

Reference	Base Polyhedron	Orientation	Partition	Transformation	Point Assignment
Alborzi & Samet 2000	Cube	Poles on face centers	Aperture 4 Square	Lambert Azimuthal Equal Area	Not Specified
Baumgardner & Frederickson 1985	Icosahedron	Unspecified	Aperture 4 Triangle (Class I)	Direct Spherical Subdivision	Not Specified
Dutton 1984	Octahedron	Octant aligned	Implied Aperture 3 Hexagon	Direct Spherical Subdivision	Class II Triangle Vertices
Dutton 1999	Octahedron	Octant aligned	Aperture 4 Triangle (Class I)	ZOT	Not Specified
Fekete & Treinish 1990	Icosahedron	Vertices at poles	Aperture 4 Triangle (Class I)	Direct Spherical Subdivision	Not Specified
Goodchild & Yang 1992	Octahedron	Octant aligned	Aperture 4 Triangle (Class I)	Plate Carree	Not Specified
Heikes & Randall 1995a & 1995b	Twisted Icosahedron	Vertices at poles	Twisted Aperture 4 Hexagon (Class I)	Optimized Direct Spherical Subdivision	Twisted Class I Aperture 4 Triangle Vertices
Sadoury et al. 1968	Icosahedron	Vertices at poles	n-frequency Hexagon (Class I)	Direct Spherical Subdivision	n-frequency Class I Triangle Vertices
Sahr & White 1998	Icosahedron	Equator symmetric	Aperture 3 Hexagon	ISEA	Cell Centers in ISEA Projection Space
Song et al. 2002	Icosahedron	Unspecified	Class I Aperture 4 or 9 Triangle	Equal Area Small Circle Subdivision	Not Specified
Thuburn 1997	Icosahedron	Vertices at poles	Aperture 4 Hexagon (Class I)	Direct Spherical Subdivision	Class I Aperture 4 Triangle Vertices
White et al. 1992	Truncated Icosahedron	Hexagon face covering CONUS	Aperture 3, 4, or 7 Hexagon	Lambert Azimuthal Equal Area	Not Specified
White et al. 1998	Icosahedron	Not Specified	Class I Aperture 4 or 9 Triangle or Class I Aperture 4 or Class II Aperture 9 Hexagon	Direct Spherical Subdivision, Gnomonic, ISEA, or Fuller/Gray	Not Specified
White 2000	Icosahedron or Octahedron	Not Specified	Aperture 4 Diamond	Not Specified	Not Specified
Wickman et al. 1974	Stellated Dodecahedron	Stellation vertex on pole	Aperture 4 Triangle (Class I)	Area-adjusted Direct Spherical Subdivision	Not Specified
Williamson 1968	Icosahedron	Vertices or Face Centers at Poles	Implied Class II Aperture 4 Hexagon	Direct Spherical Subdivision	Modified Class II Triangle Vertices

For a fuller discussion on the potential solutions for each design choice the reader is directed to the literature cited at the end of this document. The following example from Sahr, K., White, D., and Kimerling, A. J., 2003) presents a simple overview outlining the design choices taken to construct a good general-purpose Geodesic DGGS.

First, due to its lower distortion characteristics the icosahedron is chosen as the base platonic solid. It is oriented with the north and south poles lying on edge midpoints, such that the resulting DGGS will be symmetrical about the equator.

Next a suitable partition is selected. The hexagon partition has numerous advantages, and the smallest possible aligned hexagon aperture, aperture 3, is chosen; as mentioned earlier the aperture is the number of shapes chosen to sub divide two consecutive resolutions in a DGGS.

Because equal-area cells are advantageous for many applications, the inverse Icosahedron Snyder Equal Area (ISEA) projection is selected to transform the hexagon grid to the sphere, and finally it is specified that each DGGS point lies at the center of the corresponding planar cell region. The resultant grid, see Figure 3–12, is termed the ISEA Aperture 3 Hexagonal (ISEA3H) DGGS.

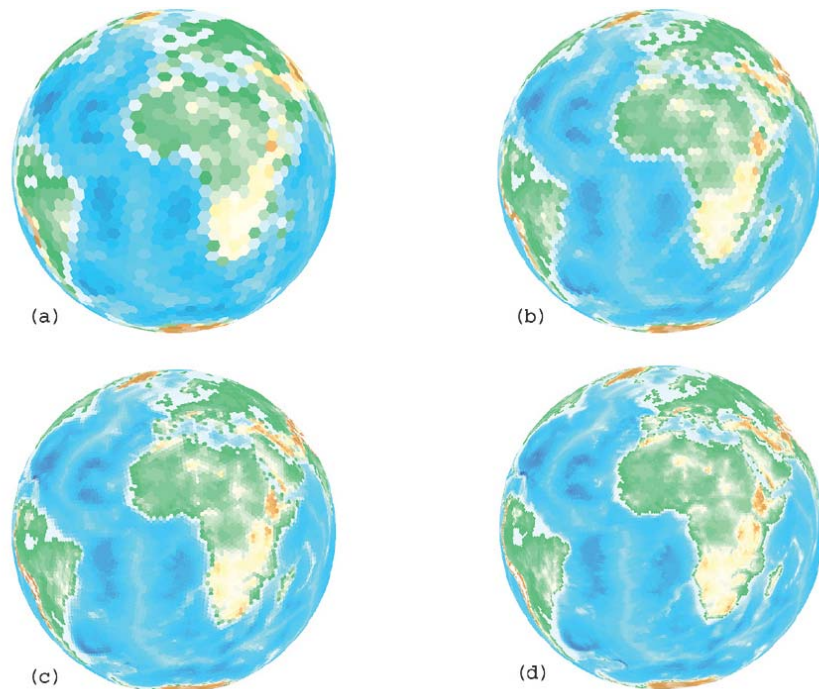


Figure 3–12.

ETOPO5 5' global elevation data binned into the ISEA3H Geodesic DGGS at four resolutions with approximate hexagon areas of: (a) 210,000 km², (b) 70,000 km², (c) 23,000 km², and (d) 7,800 km². (adapted from Sahr, K., White, D., and Kimerling, A. J., 2003)

3.4 Summary

Grids based on simple square partitioning of the globe are by far the most familiar to users and they map efficiently to common data structures and display devices. They do not have equal area cell regions with increasing distortion in area, shape and interpoint spacing as one moves from the equator. Polar singularities means that points at the north and south poles map to lines within this grid system and square grid do not exhibit uniform adjacency. Grids based on adapted parti-

tioning have been successfully implemented that reduced latitudinal distortions.

Tiling of the Globe once it is in a specified projection does allow simple determination of grid point positions via forward and inverse projection transformations. Global map projections are inherently distorted and this distortion can only be addressed and reduced by the use of more complex interrupted or combined projections.

Using a platonic solid to represent the Globe and then subdividing the faces of the solid with a regular polygon generates a DGG with uniform cell dimensions. The cell dimensions cannot be defined but are determined on best fit alone. The generation of a Geodesic DGG is complex, as is the relationship between cell and geographic locations. Whilst tiling or partitioning may be implemented on an ellipsoid definition of the Globe the Geodesic DGGs can only, currently, be implemented upon a sphere.

4 Candidate Grids

In the following section four candidate DGG's are presented. The first two candidate grids were selected since they are the two current operational grids used within IPF and the later grids were selected as the first represents the most commonly used DGG's for handling of earth observation data, and the final DGG is selected as this is the proposed DGG to be used for the future Soil Moisture and Ocean Salinity (SMOS) mission. Specifically the candidate DGG's are; the WARP4 grid, which is the current DGG implemented within WARP 4.0; the QSCAT grid, an IPF proprietary grid used within operational processing of NASA's QuikSCAT data; the EASE, Equal-Area Scalable Earth grid; and the proposed SMOS grid.

4.1 The WARP4 Grid

The discrete global grid used in WARP 4.0 for ESCAT data aggregation is an adapted version of a sinusoidal global grid (Wagner, W., 1998). The grid is generated by an adapted partitioning of the globe. First, a series of latitude small circles are created, equally spaced with a central angle of 0.25° in the south-north direction along any meridian, starting with the south pole (Fig 4-1 a). A spherical Earth with radius $r = 6370$ km is assumed, yielding a constant spacing between the latitude circles of $6370 \cdot 0.25 \cdot \pi / 180 \approx 27.79$ km, required by the processing of ESCAT data (Scipal, K., (2002)). Equation 4-1 gives the latitude of each such small circle.

$$\lambda_j = -90 + 0.25 \cdot (j - 0.5), \quad 1 \leq j < 4 \cdot 180, \quad j \in \mathbb{N} \quad 4-1$$

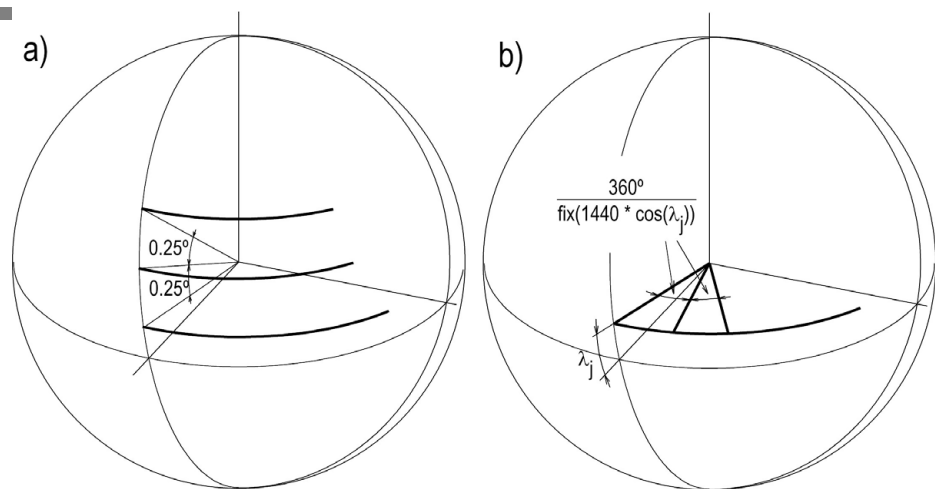


Figure 4-1.

Definition of the WARP4.0 discrete global grid. The 'fix' function denotes decimal truncation. (Adapted from Bartalis, Z. 2005)

In the longitudinal direction, the Equator is also divided into 0.25° longitude intervals, giving $4 \cdot 360 = 1440$ divisions. Each latitude circle is then subsequently divided into $1440 \cdot \cos \lambda_j$ divisions, ensuring the same 27.8 km spacing in the west-east direction as well, subject to slight variations due to decimal truncation (see Fig.4-1b). The number of grid points on each latitude circle decreases thus with increasing latitude and thus addresses polar problems as noted by Sahr, K., White, D., and Kimerling, A. J., 2003 and reducing areal distortion at higher latitudes. Equation 4-2 gives the longitude of the grid points on each of the latitude circles:

$$\varphi_{i,j} = -180 + 0.25 \cdot \frac{(i-0.5)}{\cos \lambda_j}, \quad 1 \leq i < 4 \cdot 360 \cdot \cos \lambda_j, \quad i, j \in \mathbb{N} \quad 4-2$$

The ESCAT grid covers the land surface of the Earth with more than 180000 single grid areas.

4.1.1 Grid Summary

Table 4-1

WARP4 grid summary

Grid Name	WARP4	
Ellipsoid	Sphere with fixed Radius 6370Km	
Type	Partitioned: Adapted Sinusoidal Grid	
Dimension	Latitude	Longitude
Extent	90.0 S : 90.0 N	180.0 W : 180.0 E
Delta	0.25°	0.25°
Number Elements	720	1440 (max)

4.2 The QSCAT Grid

In geographic coordinates, as used by ESCAT grid, the Earth is assumed to be a perfect sphere with a radius equal to its equatorial radius. The geodetic (or ellipsoidal) coordinate system takes into account the Earth's oblateness. To process SeaWinds scatterometer data a global grid based upon geodetic coordinate system, (see Fig.4-2.) modelling the Earth as an ellipsoid, was adopted (Kidd, R.,A, 2003).

This global geodetic grid, hereafter termed the QSCAT grid, uses the Geodetic Reference System 1980 (GRS 80) ellipsoid definition of the Earth with an equatorial radius (a) of 6,378.137 km and polar radius (b) of 6,356.752 km.

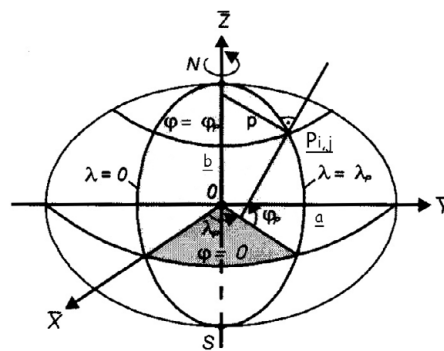


Figure 4-2.

Geodetic coordinates of latitude and longitude, from Torge, W, 2001.

A fixed grid spacing, D , between grid points $P_{i,j}$ in both the latitudinal (φ) and longitudinal (λ) sense, of 10 km is used ($D = dG = dL = 10km$). The grid points are defined from latitude of 89°S to 89°N around the circumference of globe. A fuller mathematical treatment for derivation of formulae used to define this global geodetic grid can be found in Torge, W, 2001 and Bretterbauer, K.

To generate the grid a two step approach is implemented:

- The discrete values for all latitudes ($-89.0 \leq \varphi_j \leq 89.0$) as a function of Gaussian radius, R , current position on ellipsoid surface, and grid spacing, D are calculated. This is given in Equation 4-8.
- For each latitude value calculate the discrete longitude values, based upon current position on ellipsoid and grid size. This is given in Equation 4-12.

The ellipsoid is defined with the semi-major axis, a , and the semi-minor axis, b . The eccentricity, e , of the ellipsoid is from Equation 4-3.

$$e = \sqrt{a^2 - b^2} / a \quad 4-3$$

The radius of curvature in the meridian, M , and the radius of curvature for parallels, N , are given by Equation 4-4 and Equation 4-5.

4.3 The EASE Grid

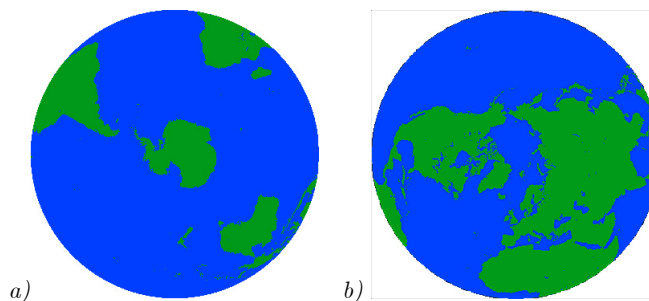
The Equal-Area Scalable Earth Grid (EASE-Grid) was the result of a NASA request in 1989 to the American scientific community on the best methods to construct geophysical products over land derived from the DMSP SSM/I (Defense Meteorological Satellite Program - Special Sensor Microwave Imager) satellite data.

Its prime use was for distributing global SSM/I data products by the National Snow and Ice Data Center (NSIDC). The grid was created by the NSIDC, University of Colorado and the University of Michigan Radiation Laboratory (RADLAB), designed to suiting the specific needs of SSM/I data, but with a potential for general application to any global scale data set.

The development of the grid was completed by 1995 and became popular amongst other polar data set producers and was implemented for AVHRR, SMMR and TOVS Path-P Polar Pathfinder data sets as well as the Arctic and Antarctic Research Institute (AARI) Sea Ice Observations. The Aquarius mission for ocean salinity, targeted for launch in 2009, will also be distributed in this grid. In the EASE-Grid, data can be expressed as digital arrays of varying grid resolutions, defined in relation to one of three possible projections, Northern, Southern and Global.

Figure 4-4.

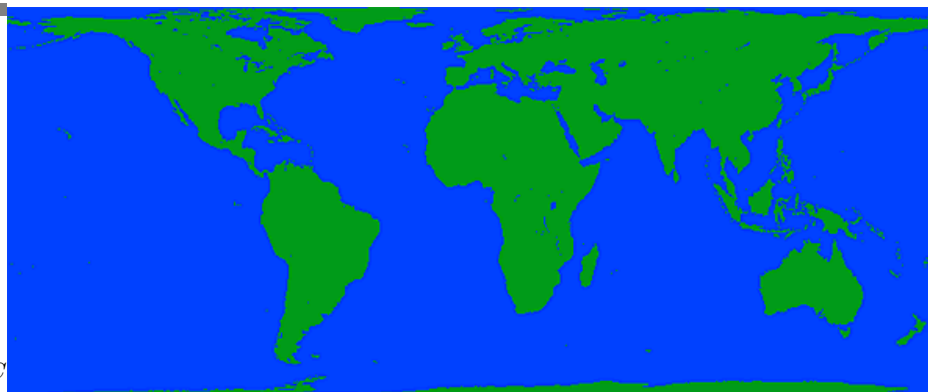
EASE polar grid projection. a) South Pole, b) North Pole. Adapted from NSIDC



The above polar projections are Lambert's Azimuthal equal-area and this Polar EASE grid, used for MODIS data is shown in Figure 3-6. The Global projection below is the Cylindrical equal-area.

Figure 4-5.

EASE global grid projection. Adapted from NSIDC



The grid is defined as a rectangular matrix on each of the projections, where each column and row can be easily matched to its lat-long coordinate. It is also possible to specify any subset area of these projections with an infinite number of possible grid definitions. This makes EASE-Grid quite flexible and in fact has been used to grid datasets with resolutions ranging from 1.25km to 250km. The cell shape is a projected “square” of the desired resolution (i.e. 25km by 25km), and the closest cells are those immediately above, below, left and right. It is a grid that is well suited for polar products, but not when the consolidation of products must be made from pole-to-pole.

Row and column positions are computed differently for each of the possible projections, thus marking EASE as a non-global Earth grid.

As an example the formulas for column (r) and row (s) position within the global cylindrical equal area projection are presented below along with the scales along meridians (h) and parallels (k). Latitude is denoted by φ and longitude by λ .

$$s = s_0 + \frac{R \sin(\varphi)}{C \cos(\varphi_0)} \quad 4-13$$

$$r = r_0 + \frac{R}{C} \lambda \cos(\varphi_0) \quad 4-14$$

$$h = \frac{\cos(\varphi)}{\cos(\varphi_0)} \quad 4-15$$

$$k = \frac{\cos(\varphi_0)}{\cos(\varphi)} \quad 4-16$$

R is the spherical Earth radius, φ_0 is the standard parallel (30°), C is the nominal cell size, (r_0) and (s_0) are the positions of the centre of the grid. These three last parameters are chosen according to the desired grid that overlays the projection. The above formulas may be inverted for each projection, to yield the formulas used to compute the lat-long coordinates of each point based on its position inside the grid.

By convention, grid coordinates (r,s) start in the upper left corner, at cell (0,0), with r increasing to the right and s increasing downward. Rounding the grid coordinates up at 0.5 yields the grid cell number. Grid cell is centered at grid coordinates (j,i) and bounded by:

$$j - 0.5 \leq r < j + 0.5 \quad 4-17$$

$$i - 0.5 \leq s < i + 0.5 \quad 4-18$$

According to Knowles, K. W., 1993 two of the most important characteristics of maps are whether they are conformal or equal-area. No map projection is both, and some are neither. On equal-area maps, a small circle placed anywhere on the map will always cover the same amount of area on the globe, and, at any point on the map, the product of the scale (h) along a meridian of longitude and the scale k along a parallel of latitude is always one. The aspect ratio $k:h$ is a measure of shape distortion.

From Brodzik, M., J. for the Northern and Southern hemisphere EASE-Grids, the aspect ratio varies from 1:1 at the pole to 1.17:1 at 45N and increases to only 2:1 at the equator. For the global EASE-Grid, the aspect ratio varies more widely from 0.75 at the equator to 24.9 at 80N. The selection of $\pm 30^\circ$ for the standard parallels of the cylindrical projection gives a map with minimum mean angular distortion over the continents. This projection is intended for the study of parameters in the mid- to low-latitudes.

The main disadvantage of this DGG is that square grids do not possess uniform adjacency and the projection exhibits distortions above mid latitudes. Its main advantages are the uniform orientation of the cells and the fact of square grids displaying very effectively on digital output devices based on square lattices of pixels.

4.3.1 Grid Summary

Since the EASE grid can be defined in any of three projections, each with a number of possible resolutions, only two of the original SSM/I grids are summarised.

Table 4-3

EASE, Global, 25km (nominal) grid summary (grid also available at 12.5km)

Grid Name	EASE (global)	
Ellipsoid	Sphere of radius of 6371.228Km	
Type	Tiled Grid; Cylindrical equal-area	
Dimension	Latitude	Longitude
Extent	86.72S, 86.72N	180.00W 180.00E
Delta	25.068 km (at 0N)	25.068 km (at 0N)
Number Elements	586	1383

Table 4-4

EASE, hemispheric-north 25km (nominal) grid summary (grid also for southern hemisphere and both available at 12.5km)

Grid Name	EASE (hemispheric -north)	
Ellipsoid	Sphere of radius of 6371.228Km	
Type	Tiled Grid; Azimuthal equal-area	
Dimension	Latitude	Longitude
Extent	0.34S, 90.00N	180.00W 180.00E
Delta	25.068 km (at 0N)	25.068 km (at 0N)
Number Elements	721	721

4.4 The SMOS Grid

The proposed grid recommended for implementation for SMOS data was selected to fulfil the following two main requirements. The first requirement was to maintain full information content of the measured SMOS samples corresponding to a maximum instrument resolution of 30km. This requirement translated to the necessity to select a uniformly spaced global and isotropic grid at twice the instrument resolution of 15km.

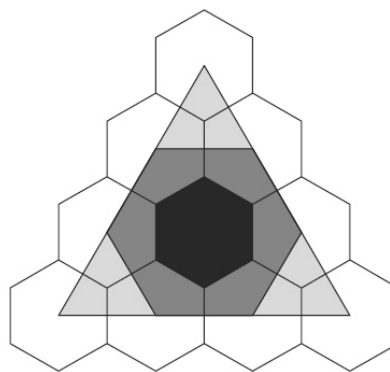
The second requirement was to minimise interpolation error due to regriding to arbitrary user defined grids. This can be achieved by having a uniform intercell spacing.

After a comparison of a number of DGG's Sues, M., Matos, P., Gutierrez, A., Zundo, M., and Martin-Neira, M., 2004 selected the Icosahedron Snyder Equal Area (ISEA) Aperture 4 Hexagonal (ISEA4H) DGGS as the prime candidate.

As noted by Carr, D., Kahn, R., Shar, K., and Olsen, T., 1997 ISEA grids are simple in concept. Begin with a Snyder Equal Area projection to a regular icosahedron inscribed in a sphere. In each of the 20 equilateral triangular faces of the icosahedron inscribe a hexagon by dividing each triangle into thirds, noted by the larger gray hexagon in Figure 4–6. Then project the hexagon back on to the sphere using the inverse ISEA projection. This yields a coarse resolution equal area grid called the resolution 1 grid. This consists of 20 hexagons on the surface of the sphere and 12 pentagons centred on the 12 vertices of the icosahedron, resulting in a global coverage of 32 cells.

Figure 4–6.

Subdividing the faces of a regular icosahedron: gray and black hexagons represent central hexagons for resolution 1 and 2 respectively. Adapted from Carr, D., Kahn, R., Shar, K., and Olsen, T., 1997



Higher resolution grids are formed by tessellation of each equilateral triangle by more hexagons and then the inverse projection is used to map these back to the sphere. The location of the central hexagon is always centred about the centre of each equilateral triangle, and the complete DGG for each resolution will always include 12 pentagons located at the vertices of the icosahedron.

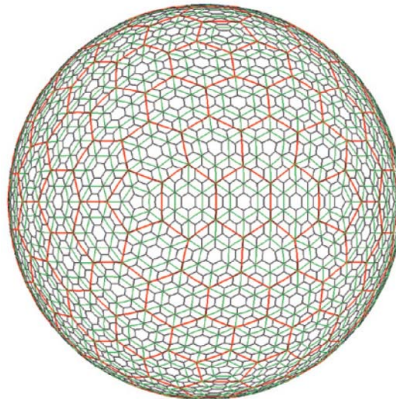
The DGG can be specified based upon the choices used to satisfy the design choices as outlined in Section 3.3. The ISEA4H DGG is constructed with the icosahedron and the base platonic solid; oriented so that the DGG is symmetrical about the equator; uses a hexagonal partitioning; transformation is achieved with the ISEA projection, and each DGG point lies at the centre of each planar cell region. The planar cell dimensions are summarised in Table 4–5 noting that since the size of the hexagon is only determined by the resolution of the grid, and therefore by the number of subdivisions of each face, the cell dimension cannot be explicitly set.

		Inter Cell Distance (km)				
Aperture	Resolution	Max	Min	Range	Mean	Std Dev
4	9	16.654	12.952	3.702	15.072	0.954

The main problems noted with this DGG are that the DGG is not congruent, therefore a new DGG must be generated for each level of resolution required, and the hexagonal partitioning on ISEA projection requires either solution of complex forward and inverse projection formulas to resolve Cartesian to Geographic coordinates.

Figure 4–7.

Icosahedron based DGG selected for SMOS. ISEA aperture 4 hexagon. Correct resolution (9) not shown. Adapted from Sahr, K., White, D., and Kimerling, A. J., 2003



4.4.1 Grid Summary

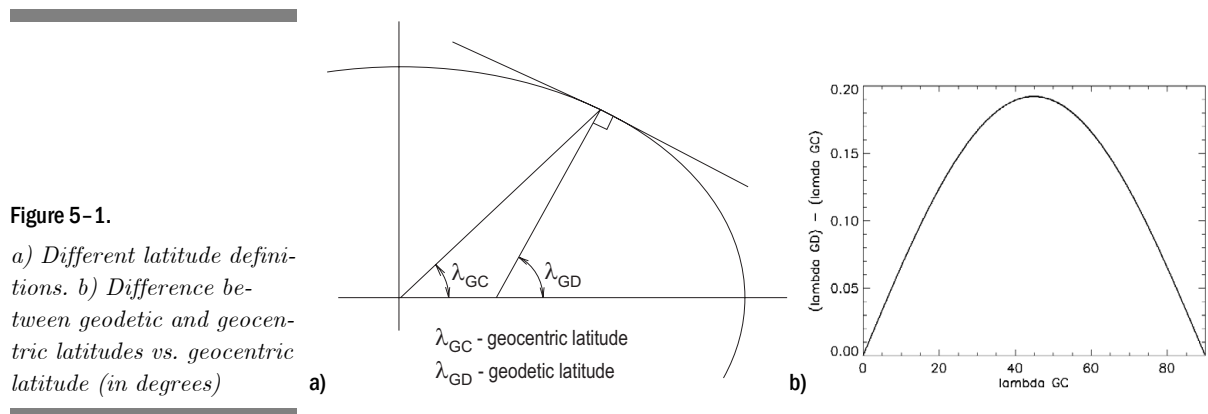
Grid Name	SMOS	
Ellipsoid	Sphere, WGS84	
Type	Regular Subdivision: ISEA4H	
Dimension	Latitude	Longitude
Extent	90S,90N	180W,180E
Delta	15.072 Km (mean)	15.072 Km (mean)
Number Elements	Total 2621442	

5 Considerations for Grid Generation and Use

5.1 Ellipsoid or Sphere

For many purposes, modelling the Earth as a sphere is adequate. Mathematically, the Earth is not the shape of a perfect sphere, but rather is slightly flattened at the poles, and has other irregularities. The largest drawback in the present WARP 4.0.grid implementation, the ESCAT grid, is considered to be the modelling of an ellipsoid by a sphere.

The Figure 5-1 presents the differences between the ellipsoid-based so-called geodetic latitude and the geocentric (geographic) latitude of the spherical model. The maximum difference occurs at 45° latitude and its value (~0.192°) is comparable to the spacing of the latitude circles of the ESCAT grid used in WARP 4.0 (0.250°). The geodetic latitude calculation is based upon the GEM6 (Goddard Earth Model 6) reference ellipsoid which has an equatorial Earth radius of 6378.144 km and a polar Earth radius of 6356.759 km ESA, 1992



One of the requirements for the new DGG is that it should be presented in the same coordinate system as the input satellite data to minimise coordinate transformation and data location errors. Currently UWI products, or ESCAT data, (within the Advanced Scatterometer Processing System asps), are generated with a ground range projection on a curved Earth surface as given by the GEM6 Earth model. Model-

ling the Earth as an ellipsoid based upon the GEM6 model would therefore satisfy this requirement.

5.2 Point Location and Grid Indexing

As noted in Section 1.1 the requirement for near real time product generation implies that there must be an efficient method for grid indexing, or point location that allows for straightforward and timely retrieval of grid data. Grid indexing refers to the generation of a unique identifier for each grid point within the DGG. Point location can refer to either the solution of the transformation for input data coordinates to grid coordinates, or from a grid coordinate to its neighbouring grid points.

For DGGs generated either by the partitioning or tiling methods point location requires the simple solution of a transformation, or projection equation. It can be easily seen that inversion of equations 4-1 and 4-2 will map longitude and latitude (λ, ϕ) to grid row and column (i, j) values, or the solution of equations 4-13 and 4-14 will directly generate row and column (r, s) indices from longitude and latitude values. Conversely these equations can be used to retrieve longitude and latitude from grid (row and column) coordinates.

For DGGs generated by subdivision point location naturally requires a more complex transformation, where the transformation must account for the base platonic solid, the orientation of the solid and the solution of the transformation equations from the face to the sphere. As noted by Sahr, K., 2005, (*pers. comms*) for the ISEA family of DGGs the primary inefficiency is the solution of the ISEA projection.

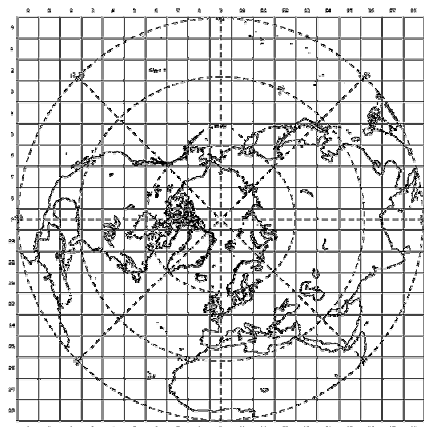


Figure 5-2.

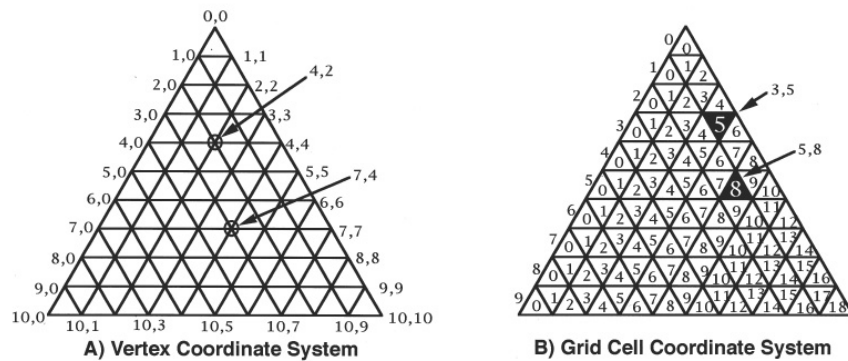
*EASE polar grid index,
Adapted from NSDIC*

Grid indexing, or grid addressing, has similar levels of complexity depending upon the method used to generate the DGG. It is straightforward to generate unique indices for DGGs generated by partitioning or tiling, with the indexing of a tiled grid being the simplest to imagine, as is shown in Figure 5-2 with the EASE polar grid. Tiles are 10

degrees by 10 degrees. Half of the tiles (313) are in the north polar grid, and the other half in the south polar grid. The north polar grid tile coordinate system starts at (0,0) (horizontal tile number, vertical tile number) in the upper left corner and proceeds right (horizontal) and downward (vertical). The tile in the bottom left corner is (18,18). The south polar grid tile coordinate system starts at (0,20) and the tile in the bottom left corner is (18,38).

Figure 5-3.

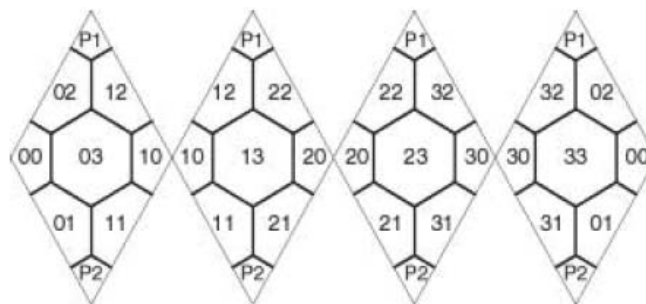
Vertex and Grid Cell indexing for a solid planar face with triangular subdivisions. Adapted from Moore, T., L., 1998



Grid indexing becomes more complex for DGGs created by subdivision. In Figure 5-3 examples of grid cell and vertex coordinate systems, Moore, T., L., 1998 , are presented. These both allow for the indexing of a single face of a planar solid with a triangular partitioning. In Figure 5-4 an addressing system for hexagons at the first level of subdivision of an octahedron is presented White, D., 2000 . For detailed explanation on the generation of these indexes the reader is referred to the cited texts.

Figure 5-4.

Addressing system for hexagons at the first level of subdivision, resolution 1, of an octahedron. Adapted from White, D., 2000



5.3 Grid Generation

Although the generation of DGGs by the method of subdivision seems quite complex there are a number of software's, made available as scientific shareware, which allow DGG generation by this method. These software's are of interest if modules are available in C++ and

therefore potentially could be integrated within the WARP operational processing chain, and if they are unconstrained by software licence agreements, such as public domain software.

One package, SCRIP, A Spherical Coordinate Remapping and Interpolation Package, is a software package which computes addresses and weights for remapping and interpolating fields between grids in spherical coordinates. It was written originally for remapping fields to other grids in a coupled climate model, but is sufficiently general that it can be used in other applications as well. The package should work for any grid on the surface of a sphere. SCRIP currently supports four remapping options. (Fortran 90). This is made available from the Climate, Ocean and Sea Ice Modeling Project (COSIM), and can be downloaded from <http://climate.lanl.gov/Software/SCRIP/index.htm>. This software was not evaluated as it is only available in Fortran 90.

Another software; DGGRID is a public domain software program specifically designed manipulating ISEA DGGs. Currently DGGRID can generate DGGs (whole earth or for user-selected regions), perform address conversions, bin point values into DGGs, and perform presence/absence binning into DGGs, Sahr, K., 2001. DGGRID was entirely written in C++ by Kevin Sahr www.sou.edu/cs/sahr/dgg/dggrid/dggrid.html.

After correspondence with Kevin Sahr, the following limitations of DGGRID are noted. The software only supports ISEA DGGs generation based on a sphere, there is no current version to support DGGs based on ellipsoids. The possible intercell distances are limited to those corresponding to grid resolution and aperture. This means that grid cell dimensions can not be explicitly set, but the best solution can only be selected from all possible alternatives. As an example the intercell distances for an ISEA3H DGG are presented in Table 5–1. All measurements are in kilometres and it is noted that the proposed SMOS grid is resolution 9 of the ISEA3H DGG (last row of the table).

Aperture	Resolution	Max	Min	Range	Mean	Std D
4	1	4003022	3526826	476196	3685558	224481
4	2	2017481	1730199	287281	1883789	121571
4	3	1024992	853056	171936	953059	61380
4	4	520746	422253	98493	479364	30689
4	5	262559	209612	52948	240423	15304
4	6	131991	104304	27687	120401	7641
4	7	66296	51987	14308	60249	3817
4	8	33248	25941	7306	30137	1908
4	9	16.654	12.952	3.702	15.072	0.954

Table 5–1
ISEA with Hexagonal partition

Although DGGRID does allowing efficient indexing and searching from latitude longitude coordinate pairs to cell number, and from cell number to latitude longitude, the only way to retrieve neighbourhood cell numbers is using geometric brute force, which is not efficient but works for all topologies. It can be done efficiently directly from the in-

dexes within the icosahedron quadrilaterals, and this approach could be made global by using adjustments for the quadrilateral seams, but this solution is not implemented with the current version of DGGRID (version 1.4). These limitations led to this software not being further considered.

5.4 Global Coverage

The first requirement states that the grid should be provided by a single solution and should offer a global coverage. Since the soil moisture product will only ever be generated over the Earth's land surface and also not in regions that are constantly frozen, it is useful to note that in these regions the DGG will not have to offer an optimum solution in the terms of either being equal area or uniform grid spacing.

The areal extent where the soil moisture product is generated is presented in Figure 5-5 and denoted by the shaded polygons. The DGG only has to offer an optimum solution between the latitudes of 54°S and 83°N, and within these limits optimum solution should also include minimal distortion.

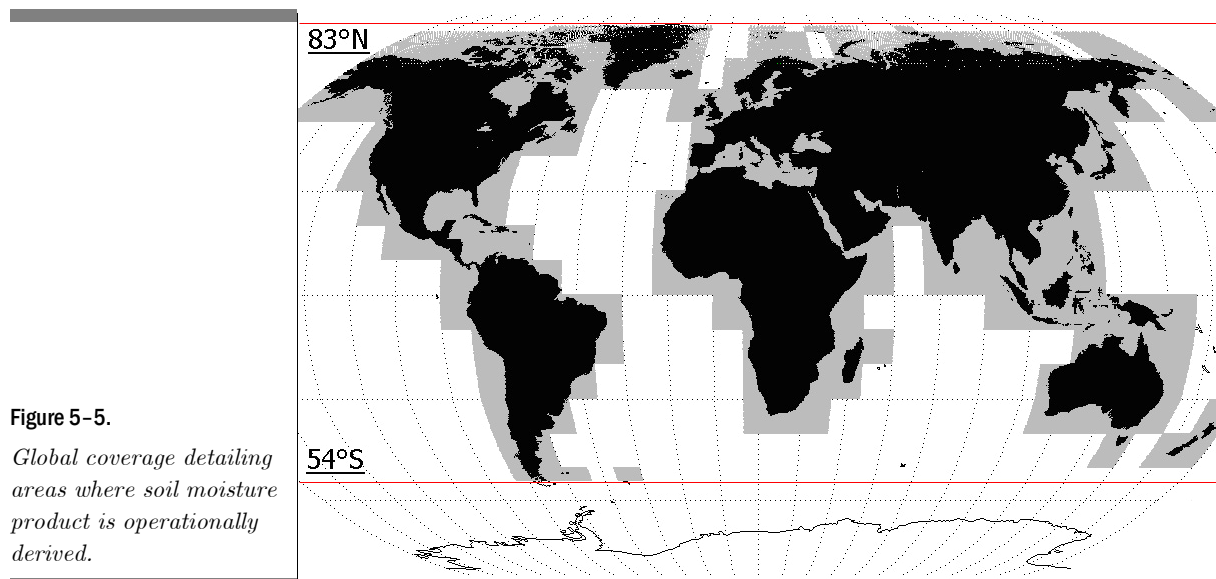


Figure 5-5.
Global coverage detailing areas where soil moisture product is operationally derived.

6 Comparison of Candidate Grids

In order to determine which of the candidate grids will offer the best potential solution for the WARP5 grid it is useful to return to the requirements stated in section 1.1 and update them in reflection to considerations made in section 5. From the initial eight requirements five are seen to remain valid, three requirements are considered redundant and a further requirement is included for consideration. These requirements are detailed in the following section.

6.1 Consideration of Grid Requirements

6.1.1 Grid Requirements

Coverage: The grid must offer a minimum complete coverage of 54°S to 83°N (see section 5.4) with minimum distortion within this extent.

Equal Area: The requirement for a uniformly spaced isotropic equal area grid at (at least) twice instrument resolution remains the same as initially stated.

Geodetic Coordinate System: The grid must be based upon the geodetic coordinate system (see section 5.1)

Grid Spacing: The requirement for uniform grid spacing remains unchanged.

Data Access: The requirement for an efficient method for grid indexing, or point location, remains unchanged.

Ease of Implementation: It is important to consider the practical implementation of the grid, and so the ease of grid implementation must be taken into account (see sections 5.2 and 5.3).

6.1.2 Redundant Grid Requirements

Resolution: Since only one resolution grid is required, and not a DGGS, it is not necessary to employ a congruent grid, but rather that data with different resolutions must be easily resampled on to the grid.

This reinforces the requirement for uniform grid spacing. The requirement for a multiple resolution grid is no longer considered.

Resampling: If the grid exhibits uniform grid spacing then it will be possible to resample data from the grid to any other meaningful grid. This requirement is no longer considered but emphasises the requirement for uniform grid spacing.

Knowledge Transfer: The requirement to make full use of IPF’s experience and knowledge concerning current grids used within IPF’s operational systems, is considered too subjective an argument to be used alone as a defining criterion in the assessment of candidate grids.

6.2 Assessment of Candidate Grids

The intention of this study was to objectively report upon the suitability of the candidate grids and present a proposal for the WARP5 grid based upon the outcome of this assessment.

As noted by Sahr, K., White, D., and Kimerling, A. J., 2003 there is no single DGG that can provide an optimum solution for all applications, and so in the DGG assessment, as with any requirement driven solution, the requirement criterion have an order of importance, and therefore a subjective weighting is applied. For example the proposed SMOS grid was based upon the requirement of a quantitative minimisation of intercell distance (Suess, M., Matos, P., Gutierrez, A., Zundo, M., and Martin-Neira, M., 2004).

In relation to the WARP5 grid is it critical that requirements concerning efficient data access, geodetic coordinate system, and ease of implementation are fulfilled.

The candidate grids in section 4 are assessed according to the requirements in section 6.1.1 and a simple compliancy matrix presents the results in Table 6-1, these results are further discussed in this section.

Table 6-1
Simple scoring of candidate grids

Requirement	WARP4	QSCAT	EASE	SMOS
Coverage	✓	✓	✗	✓
Equal Area	✓	✓	✓	✓
Geodetic System	✗	✓	✗	✗
Grid Spacing	✗	✗	✗	✓
Data Access	✓	✓	✓	✗
Ease of Implementation	✓	✓	✓	✗
Score	4	5	3	3

The main weaknesses in the current WARP4 grid are that being based upon a spherical model of the Earth it uses a geocentric coordinate system, and that it does not comply with the requirement for uniform grid spacing.

The EASE grid also fails to comply with the requirements for uniform grid spacing and coordinate system, but also since the projection of global EASE grid was designed for the study of parameters in the mid- to low-latitudes (Brodzik, M., J.) it does not offer a complete coverage of the required area with minimal distortion.

Whilst the SMOS grid does comply with uniform grid spacing, the complexity of implementation of the ISEA4H DGG, as summarised in section 3.4 and the inefficiency of data access in the retrieval of neighbourhood grid locations, as noted in section 5.3, results in this grid failing to pass critical requirements. It is also noted that since the ISEA4H DGG is based upon an icosahedron inscribed into a sphere that this grid is based upon geocentric coordinate system.

Taking into account IPF's requirements the compliancy matrix shows that the most suitable candidate grid, with the highest score, is the QSCAT grid. A proposal for the WARP5 grid, based upon the QSCAT grid is detailed in section 7.

It is noted however, that both the WARP4 grid and QSCAT grid have both been awarded negative marks concerning compliance with the requirement for uniform grid spacing. A study has been undertaken to analyse the actual variations in intergrid distances for both of these grids and the results are presented in Annex A: Intergrid Distance.

7 Proposed Grid

7.1 The WARP5 grid

The proposal for the WARP5 grid is a global adapted geodetic grid using the GEM6. It is based upon the implementation of the QSCAT grid, as described in Section 4.2, with some minor modifications.

The geodetic grid is based upon the assumption that the Earth can be accurately modelled as a rotated ellipsoid. In the QSCAT grid, by using the Gaussian Radius in the calculation of discrete latitude values, given by Equation 4-7, the radius of the Earth for any given latitude is slightly overestimated. The radius of the curvature of the meridian, M , should be used instead. Although the overestimation only has a mean of 0.34% with a standard deviation 0.11% this modification correctly adheres to the assumption that the Earth is modelled a rotated ellipsoid.

The second modification is seen in the calculation of the discrete longitude values. To clarify the calculation a less complex approach, is used as shown in Equations 7-5 to 7-7

To generate the grid the same two step approach is implemented:

- The discrete values for all latitudes ($-89.0 \leq \varphi_j \leq 89.0$) as a function of the radius of the curvature of the meridian, M , current position on ellipsoid surface, and grid spacing, D are calculated. This is given in Equation 7-3.
- For each latitude value calculate the discrete longitude values, based upon current position on ellipsoid and grid size. This is given in Equation 7-7.

The radius of curvature in the meridian, M , and the radius of curvature for parallels, N , are given by Equation 7-1 and Equation 7-2.

$$M = b^2 / (a \cdot (\sqrt{1 - e^2 \cdot \sin^2 \varphi_j})^3) \quad 7-1$$

$$N = a / \sqrt{1 - e^2 \cdot \sin^2 \varphi_j} \quad 7-2$$

The discrete latitude values, noted $d\varphi$ in Fig.4-3., can be calculated from Equation 7-3 and Equation 7-4.

$$\Delta\varphi_j = (180^\circ \cdot D) / (\pi \cdot M) \quad 7-3$$

$$\varphi_{j+1} = \varphi_j + \Delta\varphi_j \quad 7-4$$

The discrete longitude values, $d\lambda$ as shown in Fig. 4-3. for each geodetic latitude φ_j , are calculated using Equations 7-5 to 7-7

$$N_{eq} = N \cdot \cos(\varphi_j) \quad 7-5$$

$$\alpha_1 = (180^\circ \cdot D) / (\pi \cdot N_{eq}) \quad 7-6$$

$$\lambda_i = i \cdot \alpha_1 \text{ with } 0 \leq i < 360 / \alpha_1 \quad 7-7$$

But, in order to perform distance calculations from points on the ellipsoid surface, the Gaussian radius, R , for that point is required. For a known geodetic latitude, φ_j , R_j is the geometric mean of M and N , as given in Equation 7-8

$$R_j = \sqrt{M \cdot N} \quad 7-8$$

Finally, all that is required to complete the definition of the proposed WARP5 grid is the value to be used for the grid spacing, D . To correctly sample data Nyquist sampling theory states that the grid spacing should be at least twice that of the data resolution. The grid spacing is therefore set at 12.5km. This means that the grid is suitable for ASCAT data with 25km resolution.

7.1.1 Grid Summary

Table 7-1

Summary for the proposed WARP5 grid

Grid Name	WARP5	
Ellipsoid	GEM6	
Type	Partitioned: Adapted Geodetic Grid	
Dimension	Latitude	Longitude
Extent	89.0 S : 89.0 N	180.0 W : 180.0 E
Delta	12.5km	12.5km
Number Elements	1583	3207

7.2 Variation of Intergrid Distance

Since the proposed WARP5 grid is an adapted grid it is clear that it has non-uniform adjacency and the same intergrid distance will not be maintained for all neighbouring grid locations. The intergrid distance for all neighbouring 8 points around a grid location is calculated for all grid points within the proposed WARP5 grid.

Taking a 10° latitudinal band of grid locations, based upon a central latitude, a summary of the variation of mean intercell distances with

latitude is presented in Figure 7–1. The values plotted at 90S and 90N are a summary of calculations from 85S to 89S and 85N to 89N respectively, and are noted as having a central latitude of 87° in Table 7–2.

It is interesting to note that there is a significant reduction in the maximum intergrid distances centred at the equator. This value is consistent from 1.3°S to 1.3°N, and is seen to be a simple facet of quantisation.

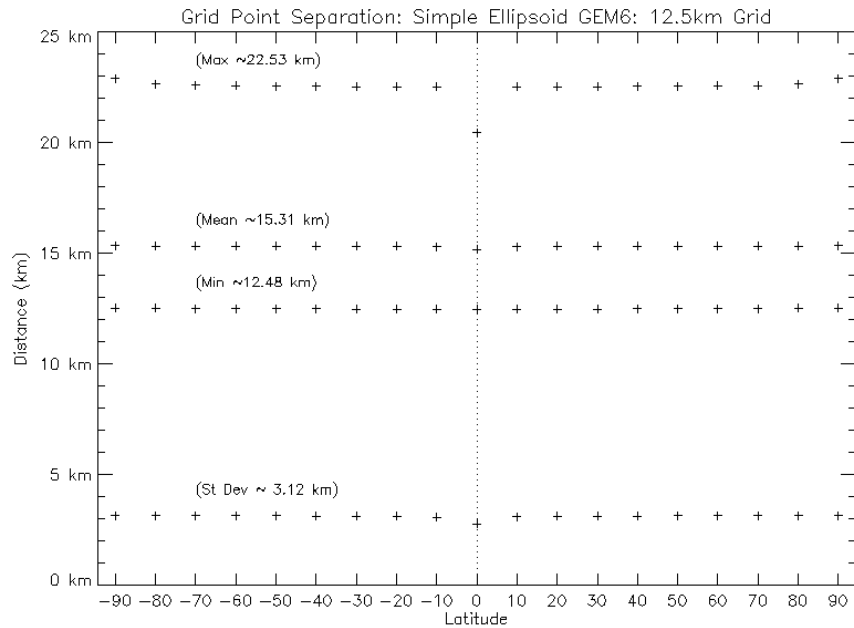


Figure 7–1.
Summary plot for WARP5 grid with 12.5km cell separation.

In Table 7–2 the actual summary values are reported for one hemisphere. In the table N represents the number of values used in the calculations for each latitudinal band.

The distribution of grid points can be likened to the centre points of a grid of regular square cells, as in Figure 2–2, but then slightly rotated about the centre point and stretched across a diagonal. The minimum distance, or the defined grid spacing, will occur between neighbouring cells in the same row that share walls whilst the maximum distance will be between those that just share vertices.

It can be seen that with the proposed WARP5 grid the mean intergrid distance is fairly stable and uniform across all latitudes.

Central Lat	Max Distance	Min Distance	Mean	St Dev	N
0.00	20446.83	12458.51	15153.07	2750.34	2278656
10.00	22510.79	12459.58	15289.42	3076.54	2219296
20.00	22516.13	12463.54	15309.57	3122.75	2142384
30.00	22523.22	12469.12	15309.79	3123.32	1974576
40.00	22531.72	12476.64	15310.36	3124.12	1746552
50.00	22542.91	12484.27	15310.62	3124.93	1465528
60.00	22555.25	12492.41	15311.47	3125.89	1139968
70.00	22573.48	12499.25	15312.65	3126.99	779928
80.00	22629.82	12501.07	15317.36	3129.74	396264
87.00	22887.11	12500.14	15341.36	3147.64	47720

Table 7-2

Summary Table for WARP5 Grid, GEM6 Ellipsoid with 12.5km Grid Spacing

Bibliography

- Anterrieu, E., Picard, B., Martin-Neira, M., Waldteufel, P., Suess, M., Vergely, J.-L., Kerr, Y., and Roques, S., 2004 A strip adaptive processing approach for the SMOS space mission. Geoscience and Remote Sensing Symposium, 2004. IGARSS '04. Proceedings. 2004 IEEE International Volume 3, 2004 Page(s):1922 - 1925 vol.3
- Bai Jian-jun, Zhao Xue-sheng, 2004 Quadtree-based indexing of hierarchical diamond subdivisions of the global. Geoscience and Remote Sensing Symposium, 2004. IGARSS '04. Proceedings. 2004 IEEE International. Volume 5, 2004 Page(s):2878 - 2881 vol.5
- Bartalis, Z. 2005. *Azimuthal Anisotropy of Scatterometer Measurements over Land*. ASCAT Soil Moisture Report Series, No. 3, Institute of Photogrammetry and Remote Sensing, Vienna University of Technology, Austria.
- Bartalis, Z. 2005. *Selection of Resampling Procedure*. ASCAT Soil Moisture Report Series, No. 6, Institute of Photogrammetry and Remote Sensing, Vienna University of Technology, Austria.
- Bretterbauer, K., Grundzüge der höheren Geodäsie. Skriptum zur gleichnamigen Vorlesung. Institut für Theoretische Geodäsie und Geophysik der TU Wien.
- Bjørke, J. T., Grytten, J. K., Hæger, M., and Nilsen, S., 2003 A Global Grid Model Based on "Constant Area" Quadrilaterals. ScanGIS 2003, pp 239-250
- Brodzik, M., J. EASE-Grid: A Versatile Set of Equal-Area Projections and Grids, http://nsidc.org/data/ease/ease_grid.html, Web Resource accessed on 01-08-2005.
- Carr, D., Kahn, R., Shar, K., and Olsen, T., 1997 ISEA Discrete Global Grids, Statistical Computing & Statistical Graphics Newsletter, Vol. 8 No 2/3 pp 31-39
- ESA, 1992. *ESA ERS-1 Product Specification*. Technical Report SP-1149, Issue 3.0. Frascati, Italy, European Space Agency.
- Hasenauer, S., Scipal, K., Naeimi, V., Bartalis, Z., Wagner, W., Kidd, R. 2005. *WARP-NRT 1.0 Reference Manual*. ASCAT Soil Moisture Report Series, No. 8, Institute of Photogrammetry and Remote Sensing, Vienna University of Technology, Austria.
- Jones, P, W., A User's Guide for SCRIP: A Spherical Coordinate Remapping and Interpolation Package, Version 1.4, Theoretical Division, Los Alamos National Laboratory
- Kidd, R.,A, 2003, Trommler, M., Wagner, W., (2003) The development of a processing environment for time-series analysis of SeaWinds scatterometer data. Geoscience and Remote Sensing Symposium, IGARSS '03. Proceedings. 2003 IEEE International, Volume 6, 21-25 July 2003 pp 4110 - 4112 vol.6
- Kidd, R. A.,2005. *NWP User Community Requirements Summary*. ASCAT Soil Moisture Report Series, No. 1, Institute of Photogrammetry and Remote Sensing, Vienna University of Technology, Austria.

- Kidd, R. A., 2005. *METOP ASCAT Data Streams and Data Formats*. ASCAT Soil Moisture Report Series, No. 2, Institute of Photogrammetry and Remote Sensing, Vienna University of Technology, Austria.
- Knowles, K. W., 1993. Points, pixels, grids, and cells -- a mapping and gridding primer. Unpublished report to the National Snow and Ice Data Center, Boulder, CO, Web Resource, <http://cires.colorado.edu/~knowlesk/ppgc.html>
- Majewski, D. and Ritter, B., 2002 Das Global-Modell GME, *Promet*, Jahrg. 27, Nr 3/4, pp 111-122, (Juni 2002)
- MIL-PRF-89020B, 2000 Performance Specification of Digital Terrain Elevation Data (DTED) 23 May 2000 Web Resource, <http://www.nga.mil/ast/fm/acq/89020B.pdf>
- Moore, T., L., 1998 A software "tool kit" in C for the application of spherical geodesic grids in paleoclimatology, *Computers & Geosciences*, Volume 24, Issue 10, December 1998, pp 965-978
- Randall, D.A., Ringler, T.D., Heikes, R.P.; Jones, P and J. Baumgardner, 2002, Climate modeling with spherical geodesic grids, *Computing in Science & Engineering*, Volume 4, Issue 5, Sept.-Oct. 2002 Page(s):32 - 41 Digital Object Identifier 10.1109/MCISE.2002.1032427
- Sadourny, R., Arakawa, A., and Mintz, Y., 1968 Integration of the Non-divergent Barotropic Equation with and Icosahedral Hexagon Grid for the Sphere, *Monthly Weather Review*, vol.96., no 6, June 1968, pp 642-653
- Sahr, K., 2001 DGGRID version 3.1b User Documentation for Discrete Global Grid Generation Software November 16, 2001
- Sahr, K., and White, D., 1998 Discrete Global Grid Systems. *Computing Science and Statistics* 30:269-278.
- Sahr, K., White, D., and Kimerling, A. J., 2003. Geodesic discrete global grid systems. *Cartography and Geographic Information Science* 30(2): 121-134.
- Scipal, K., (2002) Global Soil Moisture Retrieval from ERS Scatterometer Data, dissertation, Institute of Photogrammetry and Remote Sensing, Vienna University of Technology, Vienna, Austria
- Scipal, K., Naeimi, V., Hasenauer, S., 2005. *Definition of Quality Flags*. ASCAT Soil Moisture Report Series, No. 7, Institute of Photogrammetry and Remote Sensing, Vienna University of Technology, Austria.
- Steinwand, D.R., Mapping Raster Imagery to the Interrupted Goode Homolosine Projection, Hughes STX Corporation, Sensor Systems, EROS Data Center, Sioux Falls, South Dakota 57198, U.S.A., Web Resource, <http://edcsns17.usgs.gov/1KM/goodesarticle.html>
- Suess, M., Matos, P., Gutierrez, A., Zundo, M., and Martin-Neira, M., 2004. Processing of SMOS level 1c data onto a Discrete Global Grid. *Geoscience and Remote Sensing Symposium, 2004. IGARSS '04. Proceedings. 2004 IEEE International Volume 3, 2004* Page(s):1914 - 1917 vol.3
- Snyder, J.P. and Voxland, P.M., 1994 An Album of Map Projections USGS Professional Paper 1453 249 pp.
- Snyder, J.P., 1997 Map Projections: A Working Manual USGS Professional Paper 1395 383 pp.
- Torge, W., 2001, *Geodesy*, 3rd Edition, , Ch 4.1, The Rotational Ellipsoid, Berlin ; New York : de Gruyter, ISBN: 3-11-017072-8
- Wagner, W., 1998 Soil Moisture Retrieval from ERS Scatterometer Data, dissertation, Vienna University of Technology, Vienna, Austria

- Wagner, W., 2005. Implementation Plan for a Soil Moisture Product for NWP. ASCAT Soil Moisture Report Series, No. 5, Institute of Photogrammetry and Remote Sensing, Vienna University of Technology, Austria.
- White, D., 2000 Global grids from recursive diamond subdivisions of the surface of an octahedron or icosahedron. *Environmental Monitoring and Assessment* 64(1):93-103.
- Williamson, D., L., 1968, Integration of the Barotropic Vorticity Equation on a Spherical Geodesic Grid
- Wolfe, R.E.; Roy, D.P.; Vermote, E., 1998 MODIS land data storage, gridding, and compositing methodology: Level 2 grid *Geoscience and Remote Sensing, IEEE Transactions on* Volume 36, Issue 4, July 1998 pp 1324 - 1338
- Yang, K.; Wolfe, R.E., 2001 ;MODIS level 2 grid with the ISIN map projection *Geoscience and Remote Sensing Symposium, 2001. IGARSS '01. IEEE 2001 International* Volume 7, 9-13 July 2001 pp 3291 - 3293 vol.7
- Zhao, X.S., Chen, J., and Li, Zhilin, 2002. A QTM-based algorithm for generation of Voronoi diagrams on a sphere, In *Geospatial Theory, Processing and Applications, ISPRS Commission IV, Symposium 2002, Ottawa, Canada, July 9-12, 2002*
- Second International Conference on Discrete Global Grids (2004), Ashland, Oregon, USA, October 27-29, 2004, Web resource <http://www.discretglobalgrids.org/>

Annex A: Intergrid Distance

As noted in Section 6 both the WARP4 grid and QSCAT grid do not comply with the requirement for uniform grid spacing. To achieve equal area grids the grid point separation or intergrid distance must also be homogenous across the globe

This section assesses the variation in grid point separation for a number of global grids, based on fixed angular separation, or fixed grid spacing.

For each grid the intergrid distance for all neighbouring 8 points around a grid location is calculated for all grid points within the grid. Taking a 10° latitudinal band of grid locations, based upon a central latitude, a summary of the variation of mean intercell distances with latitude are presented as a plot and actual values, for the northern hemisphere are presented as tables.

For all grids it is interesting to note that there is a significant reduction in the maximum intergrid distances centred at the equator. This is apparent in all of these adapted portioned grids and is a simple facet of quantisation. The location of band is noted for each grid.

WARP4 Grid 0.25°

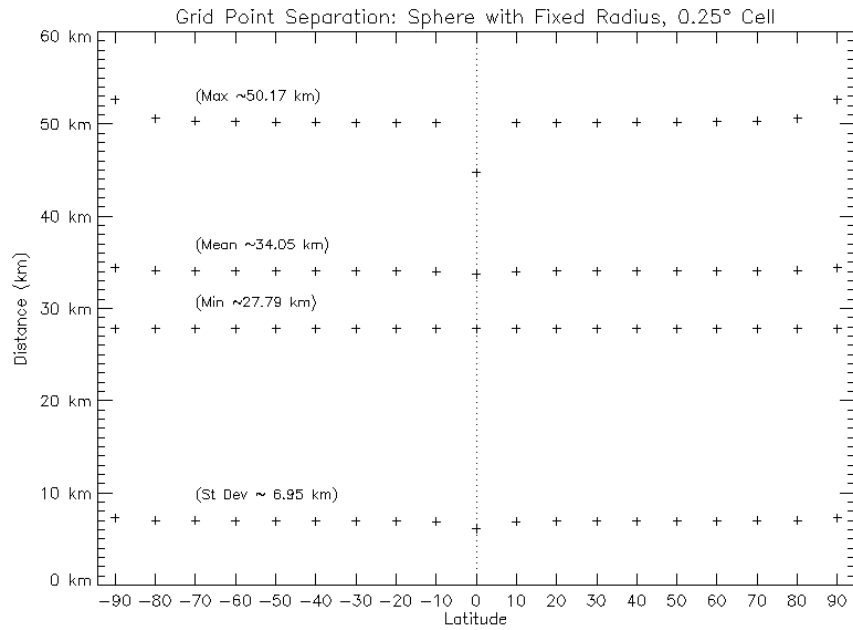


Figure 7-2.

Summary plot for WARP4 grid with 0.25° cell separation.

The reduction in the maximum intergrid distances is centred at the equator and spans 2.135°S to 2.135°N. This is equivalent to a band of approximately 17 grid cells

Central Lat	Max Distance	Min Distance	Mean	St Dev	N
0.00	44717.30	27794.26	33680.05	6073.02	459712
10.00	50128.98	27794.34	34004.92	6854.58	452728
20.00	50140.64	27794.30	34047.53	6953.49	431984
30.00	50156.32	27794.37	34049.47	6954.09	398048
40.00	50171.34	27794.28	34048.31	6953.87	352080
50.00	50207.19	27794.31	34049.74	6954.73	295360
60.00	50239.06	27794.37	34053.65	6956.55	229632
70.00	50312.49	27794.38	34063.85	6960.91	156896
80.00	50591.19	27794.61	34085.38	6975.09	79432
87.00	52654.07	27797.96	34393.17	7313.59	9789

Table 7-3

Summary table for ESCAT grid with 0.25° cell separation.

QSCAT Grid 10km

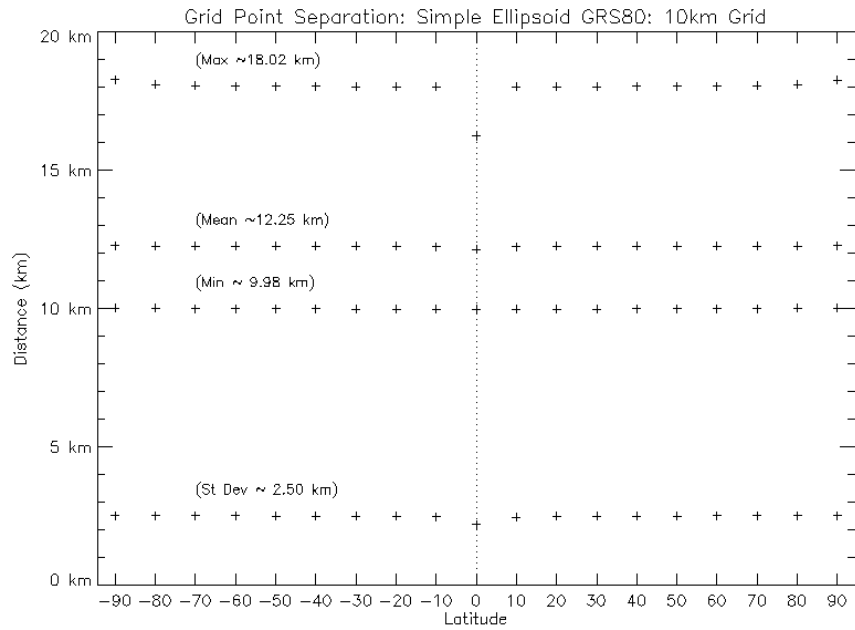


Figure 7-3.

Summary plot for QSCAT grid with 10km cell separation.

The reduction in the maximum intergrid distances is centred at the equator and spans 1.3°S to 1.3°N.

Central Lat	Max Distance	Min Distance	Mean	St Dev	N
0.00	16231.52	9965.66	12120.82	2196.52	3552856
10.00	18008.19	9966.96	12229.78	2457.50	3467832
20.00	18012.02	9970.19	12247.42	2498.09	3340296
30.00	18017.10	9974.84	12247.63	2498.57	3079352
40.00	18022.75	9980.39	12247.83	2499.12	2725056
50.00	18031.00	9986.67	12248.16	2499.78	2288272
60.00	18039.76	9993.21	12248.84	2500.55	1795912
70.00	18053.14	9999.02	12249.72	2501.36	1217496
80.00	18088.12	10000.78	12252.57	2503.08	623648
87.00	18258.37	10000.09	12267.43	2513.21	74016

Table 7-4

Summary Table QSCAT grid (GRS80 Ellipsoid) with 10km Grid Spacing

WARP4 Grid 0.125°

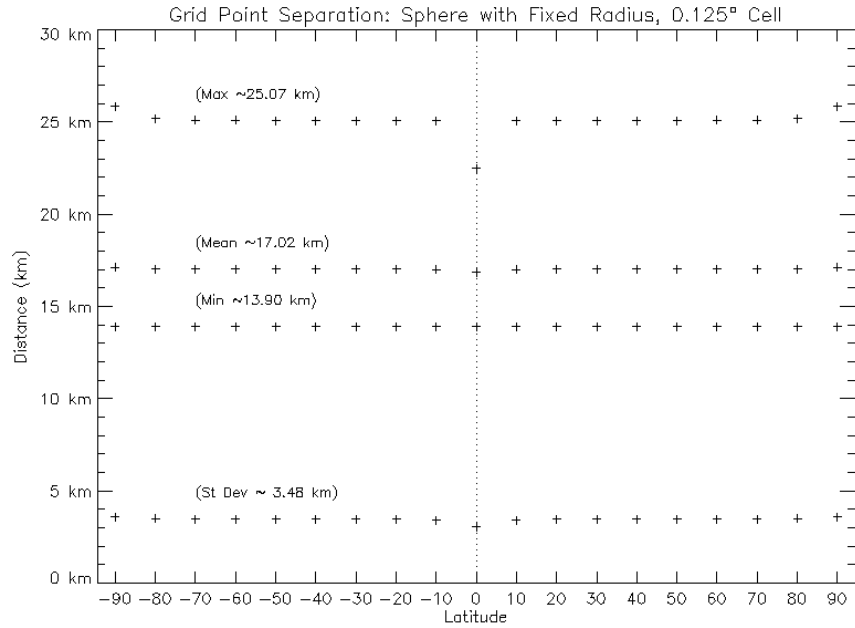


Figure 7-4.

Summary plot for WARP4 grid with 0.125° cell separation.

The reduction in the maximum intergrid distances is centred at the equator and spans 1.51°S to 1.51°N.

Central Lat	Max Distance	Min Distance	Mean	St Dev	N
0.00	22491.46	13896.66	16841.40	3043.97	1839856
10.00	25058.24	13896.71	16997.35	3419.40	1811952
20.00	25062.24	13896.53	17021.91	3475.91	1728912
30.00	25065.87	13896.78	17022.09	3475.97	1593288
40.00	25070.34	13896.98	17022.37	3476.10	1409232
50.00	25076.45	13897.09	17022.94	3476.34	1182312
60.00	25088.68	13897.11	17023.57	3476.64	919472
70.00	25108.52	13897.13	17025.42	3477.51	628640
80.00	25171.85	13897.21	17030.47	3480.42	318720
87.00	25836.36	13898.15	17121.39	3572.06	39685

Table 7-5

Summary Table for WARP4 Grid, Sphere with 0.125° Cell